

1           **STICr: An open-source package and workflow for Stream Temperature,**  
2                           **Intermittency, and Conductivity (STIC) data**

3  
4 **Authors:** Sam Zipper<sup>a,b,\*</sup>, Christopher T. Wheeler<sup>a,b</sup>, Delaney M. Peterson<sup>c</sup>, Stephen C. Cook<sup>d</sup>,  
5 Sarah E. Godsey<sup>e</sup>, Ken Aho<sup>e</sup>

6  
7 **Affiliations:**

8 <sup>a</sup>Kansas Geological Survey, University of Kansas, Lawrence KS

9 <sup>b</sup>Department of Geology, University of Kansas, Lawrence KS

10 <sup>c</sup>Department of Biological Sciences, University of Alabama, Tuscaloosa AL

11 <sup>d</sup>Department of Biology, University of Oklahoma, Norman, OK

12 <sup>e</sup>Department of Geosciences, Idaho State University, Pocatello, ID

13 \* Corresponding author: Sam Zipper ([samzipper@ku.edu](mailto:samzipper@ku.edu))

14  
15 **ORCID IDs:**

16 Zipper: 0000-0002-8735-5757

17 Wheeler: 0000-0001-9368-383X

18 Peterson: 0000-0002-3444-4772

19 Cook: 0000-0003-3642-1790

20 Godsey: 0000-0001-6529-7886

21 Aho: 0000-0001-5998-2916

22  
23 **Highlights:**

- 24       • Stream intermittency datalogger output requires substantial processing  
25       • The STICr R package provides functions to process, analyze, and QAQC this data  
26       • We share a project-wide workflow for creating FAIR stream intermittency data  
27       • In Kansas, STIC data reveal spatial stream intermittency response to geology  
28       • Temporal stream intermittency linked to precipitation and ET at different time lags

29 **Keywords:** hydrology, R, non-perennial streams, stream intermittency, Konza Prairie, FAIR  
30 data, groundwater

31  
32 *Draft manuscript submitted to Environmental Modeling & Software for peer review*  
33

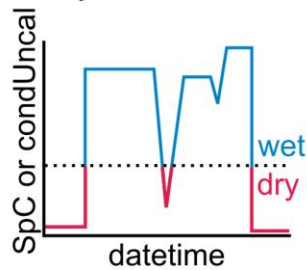
34 **Abstract**

35 Non-perennial streams constitute over half the world’s stream miles but are not commonly  
36 included in streamflow monitoring networks. Stream Temperature, Intermittency, and  
37 Conductivity (STIC) loggers are widely used for characterizing flow presence or absence in non-  
38 perennial streams. To facilitate ‘FAIR’ (findable, accessible, interoperable, and reusable) stream  
39 intermittency science, we present an open-source R package, STICr, for processing STIC logger  
40 data. STICr includes functions to tidy data, calibrate sensors, classify data into wet/dry readings,  
41 and perform quality checks and validation. We also show a reproducible STICr-based workflow  
42 for an interdisciplinary project spanning multiple watersheds, years, and research groups. In  
43 South Fork Kings Creek (Konza Prairie, Kansas, USA), we show that stream intermittency is  
44 driven by the balance between monthly precipitation inputs, seasonal evapotranspiration fluxes,  
45 and underlying geology. Overall, STICr can be used to create FAIR stream intermittency data  
46 and enable advances in hydrologic and ecosystem science.

48 **Graphical Abstract**

**STICr:** Tools for processing Stream Temperature, Intermittency, and Conductivity (STIC) sensors including tidying, calibration, classification, QAQC, and validation

*STIC data collection* → *Tidy, classified data* → *Validation against field data*



		Classified	
		wet	dry
Observed	wet	25	5
	dry	3	21

49

## 50 1. Introduction

51 Non-perennial streams represent most flowing water bodies worldwide (Messenger et al.,  
52 2021), and their prevalence in many regions has increased over the past four decades (Sauquet et  
53 al., 2021; Trambly et al., 2021; Zipper et al., 2021). Locally, the timing and spatial distribution  
54 of flow in non-perennial streams influences various ecosystem services (Kaletová et al., 2019;  
55 Stubbington et al., 2020), including carbon and nitrogen cycling (Aho, Derryberry et al., 2023;  
56 Hale and Godsey, 2019), biological community assemblages (Busch et al., 2024), ecosystem  
57 connectivity (Malish et al., 2024), and groundwater recharge (Shanafield and Cook, 2014; Zipper  
58 et al., 2022). At regional scales, non-perennial streamflow dynamics ultimately influence the  
59 quantity and quality of water available for downstream users (Brinkerhoff et al., 2024). To  
60 support effective watershed management, accurate and high-resolution *in-situ* measurements of  
61 flow intermittence are needed to quantify the hydrologic controls on connectivity and  
62 characterize impacts on water quality and society (Shanafield et al., 2020a; Zimmer et al., 2022).

63 However, non-perennial streams are underrepresented in global stream monitoring  
64 networks (Krabbenhof et al., 2022). While hydrological monitoring often focuses on  
65 streamflow, accurately characterizing low flow conditions often found in non-perennial streams  
66 is extremely challenging (Seybold et al., 2023). Additionally, streamflow is often monitored only  
67 at the outlet of a study watershed, and therefore cannot provide a detailed representation of sub-  
68 watershed variability in hydrology that can help understand hydrological processes in headwater  
69 regions and link to ecological, biogeochemical, and policy needs (Golden et al., 2025). As a  
70 result, the presence or absence of water is often used to determine hydrologic status in non-  
71 perennial streams (Sabathier et al., 2023; Jensen et al., 2019; Aho, Derryberry et al., 2023; Warix  
72 et al., 2023).

73 Stream Temperature, Intermittency, and Conductivity (STIC) loggers are a low-cost and  
74 rapidly deployable tool to monitor non-perennial flow dynamics using water presence and  
75 absence. STICs are created by repurposing the circuitry used for recording light intensity in the  
76 widely-available Onset HOBO Pendant temperature and light data logger (model UA-002-64) to  
77 provide a relative measurement of electrical conductivity using two external electrodes (Chapin  
78 et al., 2014). Since electrical conductivity of water is substantially higher than that of air,  
79 conductivity recorded by STIC sensors can be interpreted and classified to produce a binary  
80 record of water presence or absence. Recently, additional intermittency sensors such as the Smart  
81 Rock (Milford and Truong, 2024) have been developed with similar functionality to STIC  
82 loggers.

83 Leveraging data from site-specific studies of stream intermittency into regional to global  
84 understanding requires developing findable, accessible, interoperable, and reusable (FAIR;  
85 Wilkinson et al., 2016) data on stream intermittency. However, while the field of hydrology has  
86 made efforts towards improved open science practices (Hall et al., 2022; Zipper et al., 2019), the  
87 discipline has been lagging with respect to FAIR data and computational resources due to a  
88 combination of unavailable data, unclear or missing digital artifacts, and a lack of clear  
89 instructions and computational workflows (Reinecke et al., 2022; Stagge et al., 2019). Raw data

90 from STICs and other sensors requires substantial processing to develop a FAIR time series of  
91 stream intermittency. Thus, there is a need for an open, standardized, and reproducible workflow  
92 for tidying STIC data and performing basic processing operations such as calibrating measured  
93 conductivity, generating a classified wet/dry dataset, and performing quality assurance and  
94 quality control (QAQC) checks on the data.

95 To advance these goals, we present a new open-source software package (STICr) for  
96 tidying and processing STIC logger data. While many R packages exist for working with sensor  
97 data, most were developed for specific sensor types (i.e., TDPanalysis for sap flow sensors,  
98 Durand, 2020; thermocouple for temperature loggers, Gama, 2015), or to access data from  
99 specific locations and programs (i.e., TBEptools for water quality data in the Tampa Bay, Beck  
100 et al., 2021; dataRetrieval for USGS gage and water quality data, DeCicco et al., 2024). Some  
101 packages exist to perform specific functions to sensor data regardless of data type (i.e., driftR to  
102 address drift in any sensor data, Shaughnessy et al., 2018; sensorQC to perform general QAQC  
103 checks and flagging, Read et al., 2015) or for the most commonly used sensor types (i.e.,  
104 sensorstrings for HOBO, Aquameasure, and Vemco buoy sensors, Dempsey, 2024;  
105 microclimloggers for iButton and HOBO pendant sensors, Boersch-Supan and Petry, 2018).  
106 However, these packages are not equipped to handle the altered data structure of raw data from  
107 STIC sensors. Additionally, few packages exist that contain both functions for processing and  
108 tidying data as well as sensor-specific QAQC functionality. Therefore, STICr provides a FAIR  
109 framework for the entire process of data analysis for these increasingly common sensors.

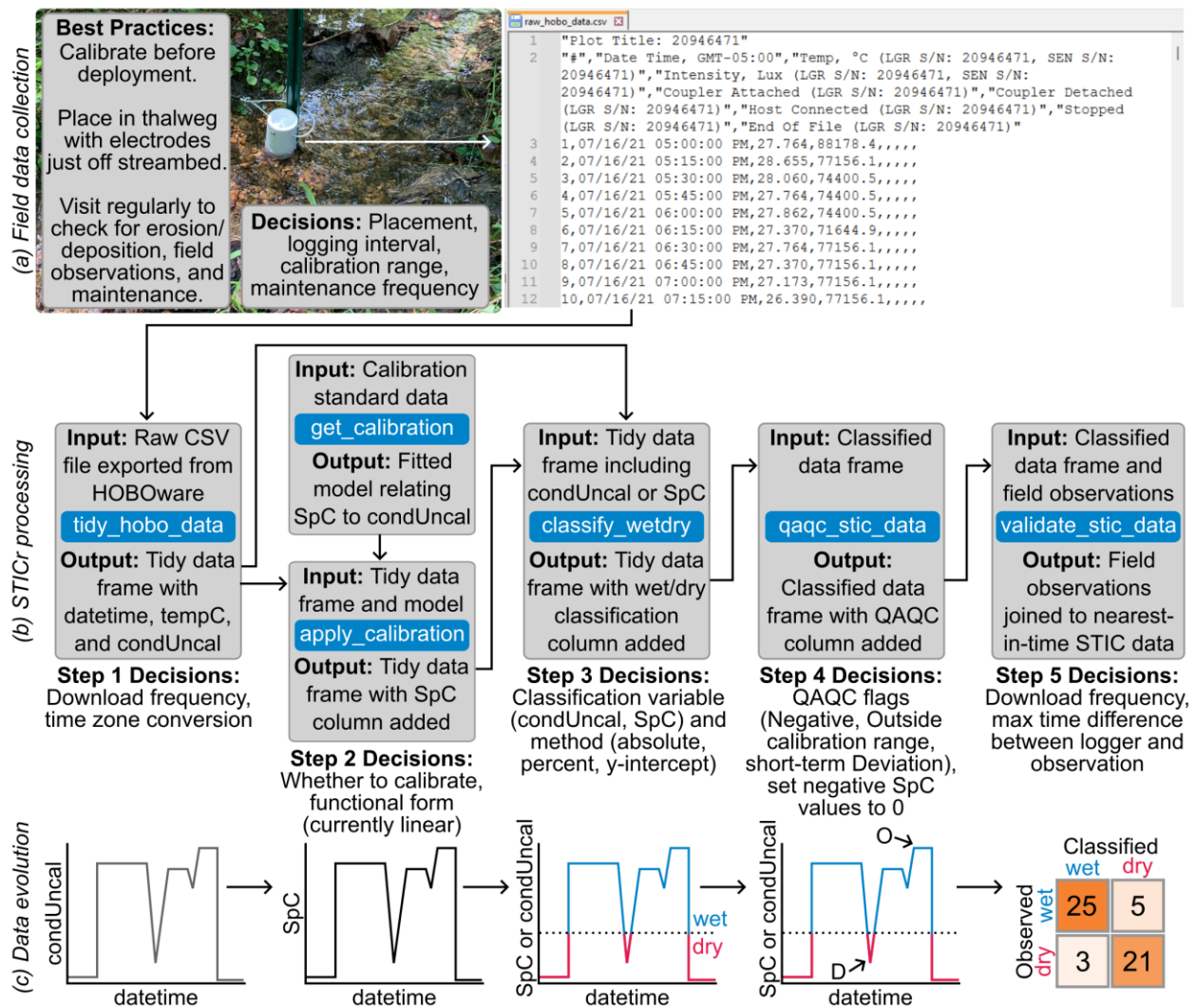
110 We first describe the core functions, inputs, and outputs within the STICr package.  
111 Following this, we demonstrate how the package can be used in a project-specific reproducible  
112 workflow that involves processing data from many loggers spread across multiple watersheds  
113 and research groups to highlight a potential application of the STICr package. We then show  
114 how stream intermittency data processed using STICr can be used to understand links between  
115 hydroclimatic processes, geological processes, and spatiotemporal patterns of stream  
116 intermittency at the watershed scale, using the South Fork of Kings Creek at Konza Prairie  
117 Biological Station as an example.

118

## 119 **2. Methods: STICr functionality**

120 The overarching goal of the STICr package is to provide a workflow spanning five data  
121 processing steps (Figure 2): (1) “tidying” the raw HOBO output files such that basic data  
122 wrangling operations (i.e., subsetting, joining, etc.) can be performed easily; (2) converting the  
123 raw conductivity measured by the sensors into calibrated specific conductivity (SpC; units  
124  $\mu\text{S}/\text{cm}$ ); (3) interpreting the conductivity data into a binary “wet/dry” classification, indicating  
125 the presence or absence of water at the sensor at each timestep; (4) providing QAQC operations  
126 such as correcting negative calibrated conductivity values and flagging anomalous classification  
127 points; and (5) validating the classified STIC data and/or calibrated SpC data against field  
128 observations. STICr also includes sample datasets showing how these data look at each step in  
129 the workflow. After these operations are performed, the resulting data should be application-

130 ready for hydrological analysis and can be more easily integrated with other datasets for analysis.  
 131 While our analysis focuses on the widely used STIC sensor, apart from the tidying function, each  
 132 of the functions and scripts we develop can also be modified to work with data from other stream  
 133 intermittency sensors such as the Smart Rock (Milford and Truong, 2024). In this section, we  
 134 briefly describe the functionality of core STICr functions including input and output within a  
 135 series of typical data processing steps shown in Figure 1.  
 136



137  
 138 **Figure 1. STICr functionality from data collection to validation.** (a) Raw data collection, including a  
 139 STIC logger deployed at a field site [photo credit: D.M. Peterson] and the resulting data after export from  
 140 the proprietary HOBOWare software. (b) Core STICr functions shown in blue boxes, including  
 141 input/output data and potential interlinkages among functions to create a processing workflow, with key  
 142 decisions for each step (described in Sections 2.1-2.5). (c) Visual depiction of how STIC data evolves as  
 143 it moves through the STICr processing workflow. Variable names used in the figure include datetime =  
 144 date and time of STIC reading, tempC = temperature in degrees Celsius, condUncal = uncalibrated  
 145 relative conductivity logged by STIC, SpC = specific conductivity, and QAQC = quality

146 assurance/quality control. ‘O’ and ‘D’ are example QAQC flags corresponding to data Outside of the  
147 calibration range and a short-term Deviation in classification (details in Section 2.4).

## 148 2.1 Step 1: Tidying output

149 When the data from a logger is initially downloaded using the Onset HOBOWare  
150 proprietary software and exported as a comma-separated value (CSV) file, it has many  
151 characteristics that make it inconvenient for analysis, including logger-specific column names  
152 with multiple spaces and punctuation marks, as well as metadata columns that do not represent  
153 actual observations (Figure 2a; example raw file available at  
154 [https://hydroshare.org/resource/6044c6b7204e4013873f13b1a502e4a0/data/contents/raw\\_hobo\\_data.csv](https://hydroshare.org/resource/6044c6b7204e4013873f13b1a502e4a0/data/contents/raw_hobo_data.csv) ). The *tidy\_hobo\_data* function takes a raw CSV file exported from HOBOWare as input  
155 and produces a tidy data frame in the R global environment and/or a CSV file, as described  
156 below. The input data frame contains three key data columns (date and time of the observation,  
157 the uncalibrated conductivity measured by the sensor, and the temperature in degrees Celsius  
158 measured by the sensor), which *tidy\_hobo\_data* preserves in the resulting output data frame. The  
159 output data frame has the following columns: *datetime*, which is the date and time of each  
160 observation; *condUncal*, which is the uncalibrated relative conductivity recorded by the STIC  
161 (unitless, though reported by HOBOWare as “Lux” from the light sensor that is modified to  
162 record conductivity); and *tempC*, which is the temperature recorded by the STIC (units: Celsius).

## 164 2.2 Step 2 (optional): Calculation of Specific Conductivity (*SpC*)

165 Since STIC sensors are created from a modified light sensor, their conductivity data  
166 output is uncalibrated conductivity (*condUncal*), which is not a physically meaningful unit. STIC  
167 sensors can monitor wet/dry conditions using their raw uncalibrated conductivity (Jensen et al.,  
168 2019), making the calibration step optional, but STIC calibration can provide more physically  
169 meaningful units (specific conductivity, or *SpC*). Calibrating sensors to obtain *SpC* can also  
170 make the STIC data more directly comparable between sensors and open new research  
171 possibilities for investigating water quality dynamics, for example through high spatiotemporal  
172 resolution mapping of solute concentrations (Paillex et al., 2020).

173 In STICr, conversion from *condUncal* to *SpC* is accomplished through two functions:  
174 *get\_calibration*, which develops a calibration curve from laboratory calibration data, and  
175 *apply\_calibration*, which applies the calibration curve to the tidied raw data to convert the  
176 *condUncal* recorded by the logger into physically meaningful *SpC*. In STICr, the *get\_calibration*  
177 function takes a data frame containing calibration data for a specific logger and outputs a fitted  
178 model object in R which relates lab-measured *SpC* to STIC-measured *condUncal*. Currently,  
179 *get\_calibration* creates a linear regression model, though other functional forms could be  
180 incorporated into the package in the future. This model object can be inspected to evaluate fit  
181 statistics ( $R^2$ , slope, intercept, etc.), uncertainty, and other properties useful to assess the  
182 performance of the calibration. The input STIC calibration data must be a data frame object with  
183 the following attribute labels: *standard*, referring to the *SpC* value (in  $\mu\text{S}/\text{cm}$ ) of a known

184 conductivity standard in which the logger was submerged for calibration, and *condUncal*,  
185 referring to the corresponding measured conductivity logged by the STIC when submerged in the  
186 solution. Typically separate calibrations are required for each STIC sensor; a standard operating  
187 procedure (SOP) for STIC sensor calibration is provided in Burke et al. (2024).

188 The fitted model produced by *get\_calibration* can then be passed as an input argument to  
189 the *apply\_calibration* function, along with the tidied data generated in Step 1, to convert the  
190 STIC time series of *condUncal* to *SpC* using the *predict.lm* function from the ‘stats’ package for  
191 R. The function returns the same tidied data frame as the input, with the addition of an *SpC*  
192 column.

### 193 2.3 Step 3: Classifying wet/dry conditions

194 The *classify\_wetdry* function supports the main purpose of STIC loggers, which is  
195 creating a binary “wet or dry” time series indicating the presence or absence of water at each  
196 measurement timestep. The principle behind generating this data set is that conductivity (either  
197 *condUncal* or *SpC*) will be at or near zero when the electrodes of the sensor are in contact with  
198 air and will be at a high value if the electrodes are in contact with water. Despite the simplicity of  
199 this concept, there are several confounding factors that complicate this binary classification.  
200 These factors include the range of stream water conductivity conditions or the possibility that  
201 loggers may become buried in moist soil, both of which may lead to difficulty in determining an  
202 appropriate wet/dry classification method.

203 STICr’s *classify\_wetdry* function takes a tidied STIC data frame as input, such as one  
204 generated by *tidy\_hobo\_data* or *apply\_calibration*. The user can then decide what column they  
205 would like to use for classification using the *classify\_var* input, which should be a variable that is  
206 highly sensitive to differences between wet and dry conditions (typically *condUncal* or *SpC*). To  
207 account for the confounding factors described above, there are three choices of *method* for  
208 classification (shown in Figure A1): (1) “*absolute*”, where the user must specify an absolute  
209 threshold of the classification variable; (2) “*percent*”, where the user specifies a percentage of  
210 the observed maximum value of the classification variable as a threshold (Warix et al., 2021),  
211 which can help account for sensor-specific differences in *condUncal* readings; or (3) “*y-*  
212 *intercept*”, in which the y-intercept of the fitted model developed in *get\_calibration* is used as a  
213 first-order approximation of the threshold (Bilbrey, 2024; Kindred, 2022). For each of these  
214 methods, values of the classification variable above the threshold are interpreted as wet and  
215 below the threshold are interpreted as dry.

216 The choice of the classification variable, method, and threshold are important decisions  
217 and may vary widely in different environments, as typical *SpC* values in streams can span orders  
218 of magnitude across freshwater systems due to physiographic and environmental factors (Bolotin  
219 et al., 2023). In describing our project-specific case study, we show how a sensitivity analysis  
220 and validation process can be used to determine an appropriate classification threshold and  
221 evaluate the potential frequency and direction of misclassification errors (Section 3.4).  
222 Alternately, separate thresholds for each sensor could be developed and implemented using the

223 STICr functionality. Ultimately, *classify\_wetdry* returns the same input data frame provided to  
224 the function with the addition of a new column called *wetdry*, which contains the character string  
225 “wet” or “dry” for every timestep.

#### 226 2.4 Step 4: Quality assurance/quality control (QAQC)

227 Once the STIC data are classified, the *qaqc\_stic\_data* function provides several options  
228 for typical QAQC procedures for stream intermittency data. The *qaqc\_stic\_data* takes in a  
229 classified data frame, as produced by the *classify\_wetdry* function, and allows the user to select  
230 different QAQC options that they may want to evaluate. Currently, there are three QAQC  
231 inspections available:

- 232 (1) Negative SpC values, which indicates an issue with the application of the calibration data to  
233 the field measurements. Most often the uncalibrated value associated with a negative SpC  
234 is 0, indicating a high-confidence dry reading. As such, the *qaqc\_stic\_data* function gives  
235 users the option to set any negative SpC value to 0 and, if so, flag the data with the  
236 character “C”, for “Corrected”.
- 237 (2) Conductivity value outside the range of calibration standards (e.g. the calibrated SpC was  
238 estimated at 1200  $\mu\text{S}/\text{cm}$  but the highest concentration standard used during calibration was  
239 1000  $\mu\text{S}/\text{cm}$ ). This QAQC flag is produced in the *apply\_calibration* step when the fitted  
240 model is applied to the time series of STIC data. In this case, the data are flagged with the  
241 character code “O”, for “Outside”, but the value of SpC is not changed. As shown in  
242 Section 3.3, these data can be highly suspect when compared to field observations, so this  
243 flag is critical for potential interpretations of STIC SpC data.
- 244 (3) Short-term deviation in STIC classification data (e.g., a single “wet” data point surrounded  
245 by many “dry” data points before and after), likely indicating a potential sensor or  
246 classification anomaly. The anomaly detection takes as input two parameters: *window\_size*  
247 is a numeric argument specifying the number of observations that the anomaly must be  
248 surrounded by in order to be flagged, and *deviation\_size* specifies the maximum of a  
249 clustered group of points that will be flagged as an anomaly. Such anomalies are assigned  
250 the character code “D”, for “Deviation”. Since non-perennial streams can exhibit diel  
251 cycling between wet and dry conditions (Hale et al., 2024; Newcomb and Godsey, 2023;  
252 Warix et al., 2023), defining the appropriate *window\_size* and *anomaly\_size* require  
253 knowledge of the site’s expected stream drying and wetting regimes and typical local  
254 stream intermittency dynamics (Price et al., 2024, 2021).

255 The *qaqc\_stic\_data* function returns the same input data frame provided to the function with the  
256 addition of a new column called QAQC, which contains the flagging character codes (“C”, “O”,  
257 and “D”) that the user specified, concatenated into a single string.

#### 258 2.5 Step 5: Validation

259 The *validate\_stic\_data* function takes a data frame with field observations of wet/dry  
260 status and (optionally) measured SpC and aggregates STIC sensor data for these variables for



261 STIC validation. The general purpose of the function is to test the accuracy of both the SpC  
262 conversion and classification. The input data frame of field observations must include a *datetime*  
263 column, as well as a column labeled *wetdry* consisting of the character strings “wet” or “dry” (as  
264 in the processed STIC data itself). Additionally, if independent field data on SpC were collected  
265 (e.g., with a sonde), this should be included as a third column in the observation data frame  
266 called *SpC*, and units should be in  $\mu\text{S}/\text{cm}$ . The *validate\_stic\_data* function then identifies the  
267 closest-in-time STIC sensor data (within a user-specific maximum allowed time range) and joins  
268 the relevant *wetdry*, *SpC*, and *QAQC* data collected by the STIC. Ultimately, this produces a new  
269 dataframe with columns for both the field observations (*wetdry\_obs*, *SpC\_obs*) and the  
270 corresponding STIC reading (*condUncal\_STIC*, *wetdry\_STIC*, *SpC\_STIC*, *QAQC\_STIC*). These  
271 data can then be used for a variety of different validation steps, such as accuracy assessments,  
272 sensitivity analyses, and checking of calibration performance. Examples of each of these  
273 validation applications from the AIMS project are shown in Section 3.

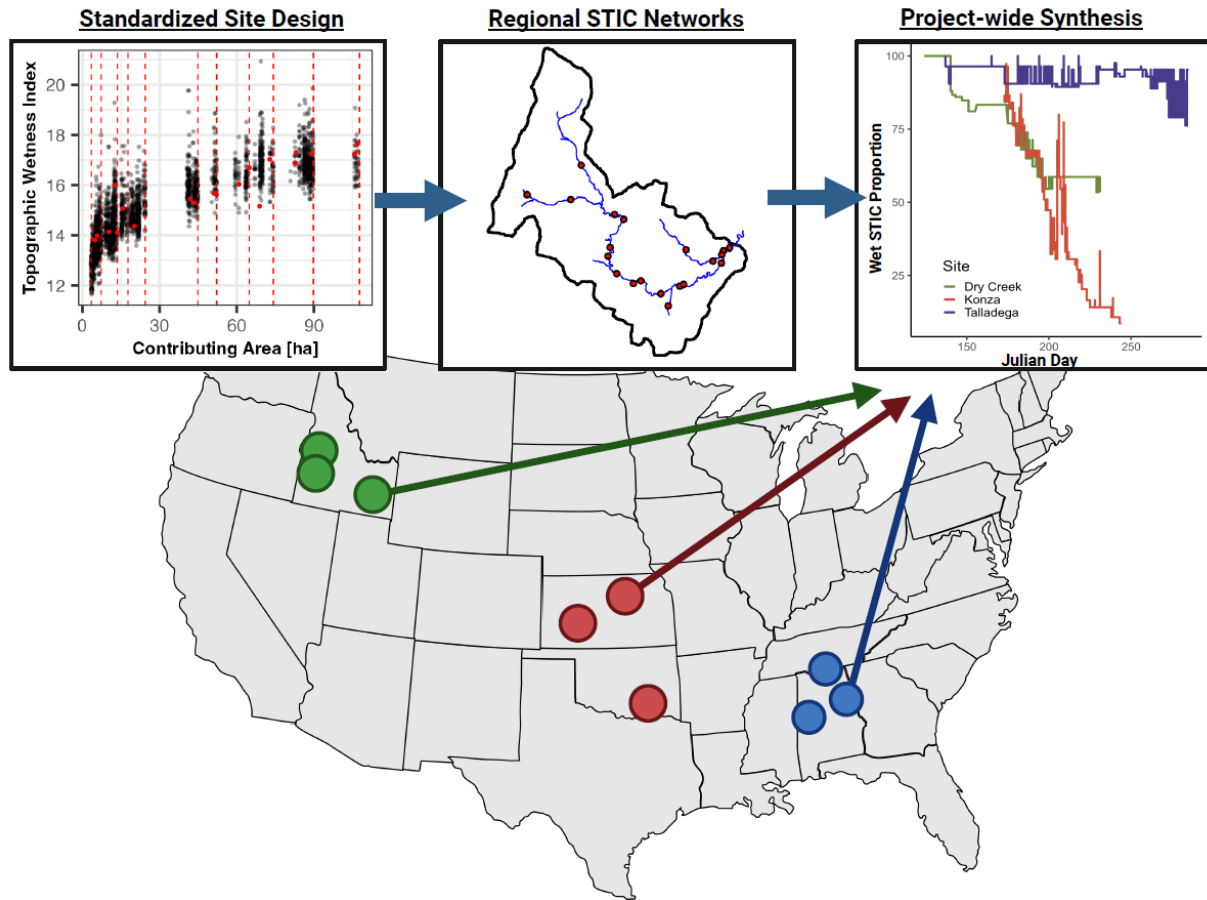
### 274 **3. Case study: Integration into project-wide reproducible workflow**

#### 275 *3.1 Stream intermittency in a cross-institution interdisciplinary project*

276 Although the functions provided in STICr provide details tidying and processing operations,  
277 their arguments and functionality remain relatively general to allow users to adapt and integrate  
278 them into reproducible workflows that fit their specific needs. Here, we provide an example of  
279 how these functions are used in a reproducible workflow for organizing and processing STIC  
280 data for the *Aquatic Intermittency effects on Microbiomes in Streams* (AIMS) project, which  
281 includes over 200 STIC loggers from nine watersheds and multiple universities, investigators,  
282 and students over a multi-year period (Figure 2; Peterson et al., 2023). AIMS is a  
283 multidisciplinary National Science Foundation-funded project (award OIA-2019603) whose goal  
284 is to collect and integrate high resolution datasets on the hydrology, biogeochemistry, and  
285 microbial ecology of intermittent streams in multiple regions of the US. As such,  
286 methodologically consistent stream intermittency data from STIC loggers form the scientific  
287 backbone of this project to interpret variations in stream dissolved organic carbon export  
288 (Bilbrey, 2024), microbiome dynamics, macroinvertebrate community structure, and many other  
289 datasets being collected. The need for consistency in processing, analysis, and QAQC of STIC  
290 data across sites and regions, as well as the need to integrate this data with other project-specific  
291 data sets (e.g., optical water quality sensors, pressure transducers, etc.), led to the development of  
292 STICr and an AIMS-specific STIC data processing workflow.

293

294



295  
 296 **Figure 2. Design of STIC data collection for the AIMS project.** Each of the circles on the map is a  
 297 study watershed where AIMS has deployed STIC sensors to monitor stream intermittency. The sequence  
 298 of plots along the top shows how a standardized site design, using topographic wetness index and  
 299 contributing area, was used to distribute the sensors within each watershed, and this consistent approach  
 300 allows for cross-site synthesis research. Top row figure sources, from left to right: Peterson; Peterson;  
 301 Kraft et al. (in prep). Figure created in BioRender. Peterson, D. (2025) <https://BioRender.com/0v4yhi7>  
 302

303 *3.2 STIC data collection best practices*

304 The first step is the collection of high-quality field data. While the focus of this paper is  
 305 data analysis, we briefly offer several recommended best practices for field deployment to ensure  
 306 high data quality (Figure 1a), and we have published SOPs on STIC deployment, maintenance,  
 307 and calibration (Burke et al., 2024; Godsey et al., 2024). Prior to deployment, we recommend  
 308 carefully calibrating the loggers using multiple solutions of known SpC that exceed the range of  
 309 expected conditions in the field. As shown below (Section 3.4), STIC SpC estimates outside of  
 310 the calibration range tend to perform quite poorly. We recommend a minimum of four  
 311 calibration points exceeding the anticipated range of SpC values that the STIC will encounter  
 312 during its field deployment, including a dry calibration point when the STIC is exposed to the air  
 313 rather than submerged in water. STICs can be re-calibrated as frequently as needed, for example  
 314 during periods when they are being collected for download and redeployment.

315 During deployment, the sensors should be placed in the stream thalweg with the sensor's  
316 electrodes just off the streambed so that it is able to sense shallow flow (shown in Figure 1a). We  
317 typically place the sensor within two millimeters of the streambed, unless rapid sedimentation is  
318 expected, in which case positioning further above the streambed helps prevent sensor burial.  
319 Along the thalweg, specific sensor locations should be targeted based on the desired hydrologic  
320 indicators for the study, for example avoiding pools if the goal is to record the expansion and  
321 contraction of the surface water network in the catchment (Jensen et al., 2019) or targeting pools  
322 if the goal is to characterize the persistence of water in the network. The STICs should be visited  
323 regularly to check for erosion or sediment deposition, and to record a field observation of the  
324 wet/dry status and SpC which can be used for validation (Godsey et al., 2024). Finally, data from  
325 the sensors should be downloaded and sensors should be maintained on a regular schedule. We  
326 recommend downloading data and changing sensor batteries every 6 to 9 months. To assist with  
327 evaluation of STIC data by other team members and researchers outside the project, we  
328 developed qualitative data quality categories, which are detailed in Appendix 1. These qualitative  
329 data quality categories are used to help other researchers interpret the reliability of the STIC  
330 measurements at a given timestep.

331

### 332 3.3 Using *STICr* to create a FAIR data workflow

333 The AIMS STIC processing workflow (Figure 3; see ‘Software and data availability’  
334 section for access) consists of five scripts written in R that make use of the *STICr* package by  
335 integrating the generalized functionality of *STICr* with additional project-specific requirements  
336 such as data naming and formatting conventions:

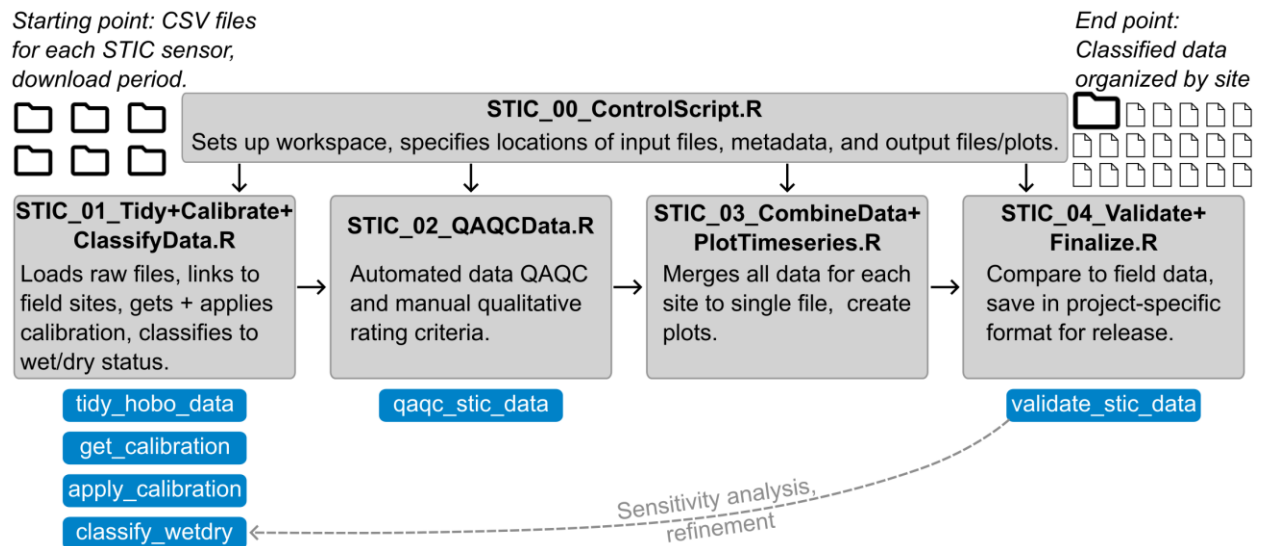
- 337 • *STIC\_00\_ControlScript.R* sets up the AIMS data processing workflow. In this script, the  
338 user defines the location of key files such as exported HOBO CSV data, a look-up table  
339 that links STIC serial numbers to specific field monitoring sites, calibration standard  
340 information, and paths to save output files and figures. Information from this control  
341 script is then read into each of the following four scripts that carry out sequential  
342 processing steps.
- 343 • *STIC\_01\_Tidy+Calibrate+ClassifyData.R* carries out the bulk of the processing,  
344 including the loading/tidying of raw HOBO CSV data (Step 1; Section 2.1), getting and  
345 applying the calibration to calculate *SpC* if available (Step 2; Section 2.2), and classifying  
346 the STIC data to create the *wetdry* column (Step 3; Section 2.3). The script uses a look-up  
347 table relating the serial number of the STIC logger to its project-specific site name  
348 (corresponding to its watershed position) to name the output files according to the  
349 project-specific convention, which contains the logger serial number, site/region codes,  
350 and the start and end date/time for the download period in YYYYMMDD HH:MM:SS  
351 format.
- 352 • *STIC\_02\_QAQCdata.R* conducts QAQC (Step 4), including the automated steps  
353 described in Section 2.4 and a manual step in which the qualitative rating criteria  
354 (Appendix 1) are assigned. The script streamlines the qualitative rating process by

355 automatically importing of digitized STIC metadata sheets from field data collection  
356 efforts and creating diagnostic graphs and tables with information from the STIC sensor  
357 (i.e., classified wet/dry conditions, SpC, and condUncal) and corresponding field  
358 observations. Plots produced by this script include time series of classified STIC  
359 *condUncal*, *tempC*, and *SpC* data, color-coded by wet/dry classification, which can be  
360 used for additional checks on classification performance. For example, the STIC daily  
361 temperature range is typically greater when the STIC is dry and exposed to the  
362 atmosphere than it is when the STIC is wet and thermal variability is dampened by the  
363 water. Therefore, paired inspection of the temperature, conductivity, and classification  
364 data can be used to assess potential misclassification issues.

- 365 • *STIC\_03\_CombineData+PlotTimeseries.R* collects the classified and QAQCed data for  
366 each site across all download periods to produce a single CSV file, and associated  
367 summary plots, of all available data for each site. This script does not use any STICr  
368 functionality, but is necessary because different STIC loggers are used at the same site  
369 during different deployments.
- 370 • *STIC\_04\_Validate+Finalize.R* script compiles field observations and uses  
371 *validate\_stic\_data* to create the validation data frame, which is then plotted in various  
372 ways including a confusion matrix, sensitivity to threshold choice for wet/dry  
373 classification, and overall accuracy (Step 5). This script also creates additional data  
374 columns and saves the data into individual CSV files for each site and year to align with  
375 the AIMS project-wide data formatting standards. The output from this script represents  
376 the final, application-ready data files that are posted to a data repository (e.g.,  
377 HydroShare; Zipper et al., 2024).

378 Overall, the AIMS STIC data workflow shows one instance of how the generalized STICr  
379 functions can be utilized for the automation of project-specific tasks.

380



381  
 382 **Figure 3. STICr as part of a project-wide data processing workflow.** The starting point of the  
 383 workflow is a set of raw CSV files exported from HOBOWare for each STIC download period. Each  
 384 processing script is shown in a gray box with a summary of key steps, and STICr functions used in each  
 385 script are shown beneath in blue. The end point is a classified and organized set of files for each site.  
 386

### 387 3.4 South Fork Kings Creek (Konza Prairie, Kansas, USA) case study

388 In this case study, we demonstrate the implementation of STICr within the project-wide  
 389 reproducible workflow to assess spatial and temporal patterns of stream intermittency in the  
 390 South Fork Kings Creek watershed (Kansas, USA). This watershed is the core AIMS study  
 391 watershed for the Great Plains region and is fully within the Konza Prairie Biological Station,  
 392 which is host to a Long Term Ecological Research (LTER) site and is part of the National  
 393 Ecological Observatory Network (NEON).

394 Streamflow in the watershed is highly intermittent and characterized by a ‘fill-and-spill’  
 395 hydrology controlled by subsurface storage dynamics (Costigan et al., 2015). There is no  
 396 pumping within the study region and both groundwater levels and streamflow are typically  
 397 highest in the late spring/early summer, which is the start of the rainy season but before plant  
 398 water use by ET reaches its peak (Gambill et al., 2024). However, there is substantial year-to-  
 399 year variability and spatial variability in groundwater-surface water dynamics (Costigan et al.,  
 400 2015). Subsurface hydrological processes are highly complex at the site due to the merokarst  
 401 landscape typical of the Flint Hills ecoregion, which consists of thinly interbedded limestones  
 402 (which act as aquifers through dissolution and fracture networks) and mudstones (which act as  
 403 aquitards, but are highly fractured and likely leaky) (Macpherson, 1996; Vero et al., 2018).  
 404 Groundwater contributes a large portion of total streamflow (Hatley et al., 2023) but subsurface  
 405 flowpaths are relatively rapid and grow longer as the stream network dries (Swenson et al.,  
 406 2024). The spatial patterns of stream-aquifer interactions are complex, as water is exchanged  
 407 between the stream and specific limestone units only in highly localized settings where  
 408 limestones outcrop onto the streambed (Gambill et al., 2024) and the merokarst groundwater

409 system has complex potentiometric surfaces that are not exclusively driven by stream-aquifer  
410 interactions (Sullivan et al., 2020).

411 While this past work suggests potential spatial and temporal heterogeneity in streamflow  
412 dynamics, these studies have primarily focused on the outlets of four tributaries of South Fork  
413 Kings Creek that have streamflow gaging stations as part of the LTER program. We installed  
414 STIC sensors at 50 locations distributed within the South Fork Kings Creek watershed in May  
415 2021, and data included in this study cover a three-year period from May 2021 to May 2024. A  
416 detailed description of site selection is presented in Swenson et al. (2024). Briefly, some  
417 locations were identified based on local hydrologic site knowledge (such as the locations of  
418 springs and confluences) while others were randomly distributed to span a range of topographic  
419 wetness index (TWI) and drainage area (Figure 2), which past work has shown to be an  
420 important control over stream intermittency in other watersheds (Warix et al., 2021). These  
421 locations were designed to balance project-wide goals related to hydrology, biogeochemistry,  
422 microbiology, and ecology, and therefore were not exclusively targeted towards stream  
423 intermittency characterization, but were driven by the overarching project goal of monitoring a  
424 gradient of stream intermittency across the watershed.

425 At each site, the STIC was installed at the thalweg of a local channel high point, such as  
426 the top of a riffle sequence, so that a “wet” STIC reading would correspond to a connected  
427 stream network at that location (as opposed to the persistence of pools at the site). Most, but not  
428 all, STICs were calibrated before deployment and STICs were downloaded and maintained  
429 approximately every 6-9 months. During these visits, and at other opportunistic occasions when  
430 project members were collecting other field data at the sites, we collected field observations  
431 including wet/dry status and independent stream water SpC, for a total of 333 field observations  
432 that can be used for validation. The STIC field data collection followed the best practices  
433 described in Section 3.2 and data were processed using the workflow described in Section 3.3.

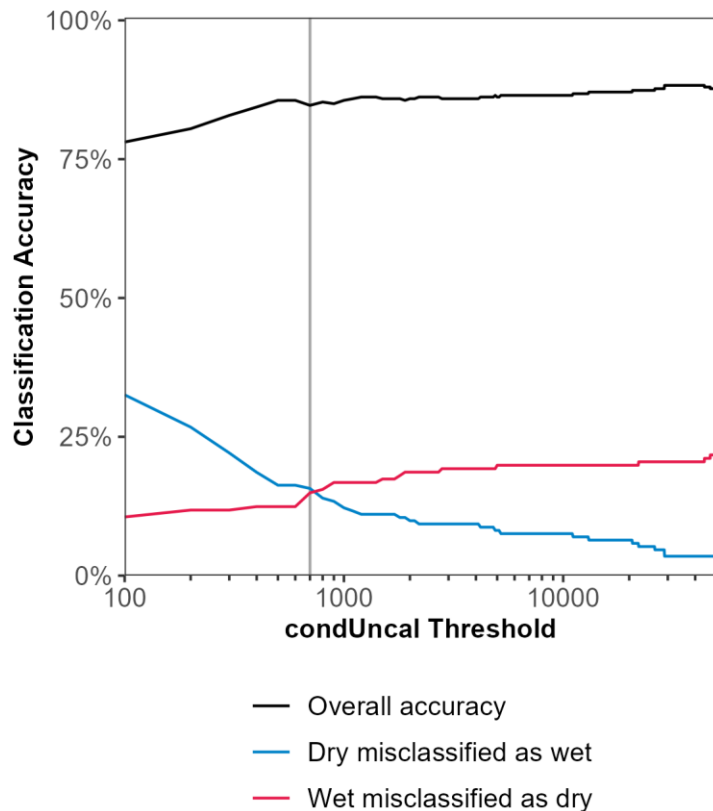
434

### 435 *3.5 STIC data sensitivity analysis and validation*

436 We conducted an iterative sensitivity analysis and validation to determine the appropriate  
437 threshold for wet/dry classification. Since we did not have calibration data for all STIC sensors,  
438 we used *condUncal* for classification. To select the *condUncal* threshold used to identify wet and  
439 dry sensor readings in *classify\_wetdry*, we conducted a sensitivity analysis by evaluating  
440 agreement with observations using unitless *condUncal* thresholds ranging from 100 to 100,000 at  
441 increments of 100. At each threshold, we calculated overall classification accuracy (percent of  
442 field observations that agree with the closest-in-time STIC wet/dry classification), the percentage  
443 of dry field observations that were misclassified as wet, and the percentage of wet field  
444 observations that were misclassified as dry.

445 We found that variability in the classification threshold had a relatively small influence  
446 on the overall classification accuracy (Figure 4), which is due to the strong conductivity contrast  
447 between air and water. However, there was an important trade-off with the type of  
448 misclassification errors, with lower *condUncal* threshold associated with a greater wet bias (dry

449 observations misclassified as wet) and higher *condUncal* thresholds associated with a greater dry  
 450 bias (wet observations misclassified as dry). For South Fork Kings Creek, we selected a  
 451 *condUncal* threshold of 700, which had a slightly lower overall classification accuracy (84.7%)  
 452 than the peak we found (max overall accuracy of 88.3% at a *condUncal* threshold of 29,000), but  
 453 minimized the difference between wet and dry misclassification errors. This threshold was  
 454 selected after consultation with other project members who plan to use the STIC data in their  
 455 analysis to balance the different types of misclassification errors and avoid either dry or wet bias  
 456 in the STIC data, demonstrating the important role of project-wide communication in developing  
 457 hydrological datasets for interdisciplinary research goals. In practice, the best classification  
 458 threshold will likely vary between sensors, watersheds, and/or regions due to variability in sensor  
 459 construction and different conductivities of stream water. Therefore, overall classification  
 460 accuracy could be improved by developing sensor-specific wet/dry classification thresholds  
 461 where resources permit, which was completed for some AIMS watersheds. STICr provides a  
 462 useful set of tools to select this threshold, apply it to the STIC data, and evaluate its accuracy.  
 463



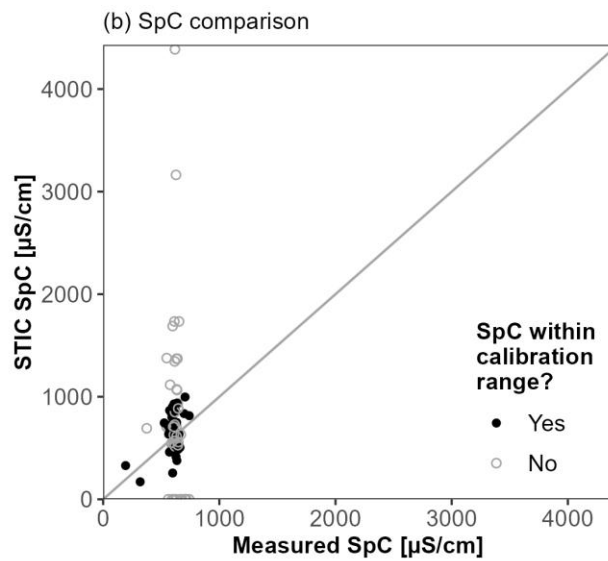
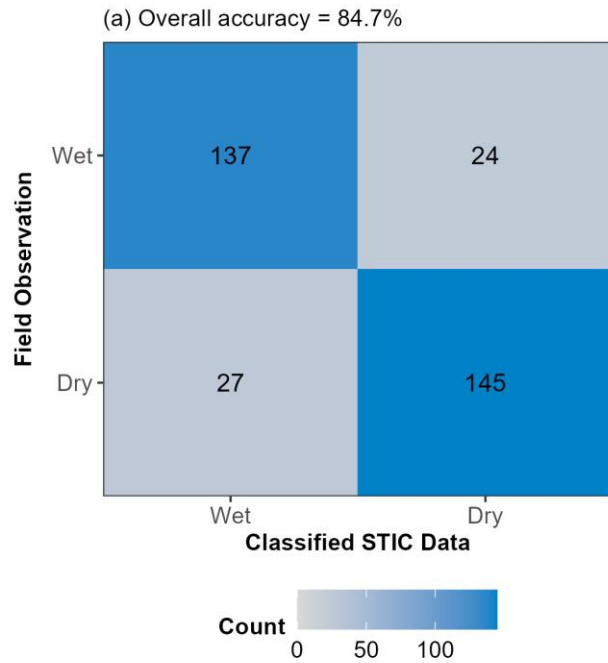
464  
 465 **Figure 4. Selecting optimal classification threshold for the South Fork Kings Creek (Konza Prairie)**  
 466 **watershed.** This figure shows the overall classification accuracy as well as the proportion of different  
 467 types of misclassification errors as a function of the *condUncal* threshold used in the *classify\_wetdry*  
 468 function. The gray vertical line (*condUncal* = 700) was used for watershed-wide classification.  
 469

470 Overall, the total classification accuracy was 84.7% and had relatively balanced data  
471 between correctly classified wet/dry conditions (137 and 145 correctly classified observations,  
472 respectively) and incorrectly classified wet/dry errors (24 and 27 observation errors,  
473 respectively) (Figure 5a). Of the 24 wet observations that were misclassified as dry, 13 of them  
474 had a *condUncal* reading of 0, suggesting that the misclassification was caused by the STIC  
475 being out of the water, for example due to channel erosion or migration. For the remaining wet  
476 observations misclassified as dry, a lower classification threshold could have fixed the issue,  
477 suggesting potential value from sensor-specific accuracy assessments and classification threshold  
478 determination.

479 However, the agreement between field-measured SpC values and calibrated STIC  
480 observed SpC data was poor, with much higher SpC values estimated from the STICs than  
481 observed in the field-measured SpC (Figure 5b). This comparison demonstrates the value of our  
482 QAQC procedures, as screening out any data points flagged with a “C” (meaning negative SpC  
483 values were obtained after calibration) or an “O” (meaning the calibrated SpC was outside the  
484 range of standards) eliminates the most extreme SpC values, which are shown as gray circles in  
485 Figure 5b. The remaining data points are distributed close to the 1:1 line (slope = 0.998), though  
486 the overall coefficient of determination remains low ( $R^2 = 0.20$ ) compared to lab fits to  
487 calibration standards, which generally had an  $R^2 > 0.9$ . The lower agreement compared to field  
488 could be due to issues with the STIC calibrations (such as calibration drift through time), issues  
489 with the STIC *condUncal* raw data (such as biofouling of the STIC electrodes during deployment  
490 which could influence conductivity readings), or issues with the field observations (such as  
491 errors in portable water quality sondes used to measure SpC in the field). Through this validation  
492 process, we can constrain the potential applications of STIC-derived SpC data and identify  
493 potential opportunities to improve future calibration and data collection practices.

494





495  
496  
497  
498  
499

**Figure 5. STIC data validation from the South Fork Kings Creek (Konza Prairie) watershed.** (a) Confusion matrix showing classification accuracy. The numbers correspond to the total number of observations in each quadrant. (b) Scatterplot showing calibrated SpC accuracy.

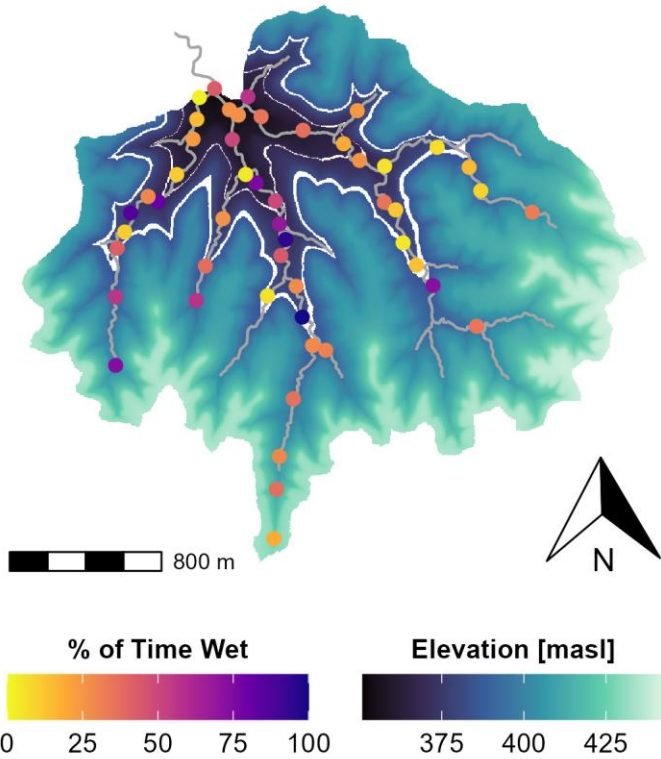
500 *3.5 Spatial and temporal variability in stream intermittency*

501 Our STIC data collection, which was motivated by the goal to develop improved  
502 understanding of spatial patterns of stream intermittency at a watershed scale (Section 3.1),  
503 revealed both spatial and temporal of stream intermittency dynamics in South Fork Kings Creek.  
504

505 *3.5.1 Spatial patterns of stream intermittency*

506 We observed that the South Fork Kings Creek watershed generally has the most flow  
507 persistence (defined as the greatest percent of time wet) in the middle reaches of the westernmost  
508 tributaries in the study area (Figure 6). In contrast, flow persistence is lower in the upstream and  
509 downstream portions of the western tributaries as well as the easternmost tributaries. However,  
510 there is substantial reach-scale variability within these broad patterns, and we observed STICs  
511 that are usually wet within 100s of m of STICs that are usually dry. While the study watersheds  
512 have different burn frequencies, this does not appear to be a major driver of hydrological  
513 differences documented by our STIC sensors, as the easternmost two watersheds are burned at  
514 one-year and twenty-year intervals, and therefore represent endmembers with respect to fire  
515 regimes and woody vegetation encroachment (Keen et al., 2024), yet exhibit similar stream  
516 intermittency dynamics.

517 Instead, we attribute the spatial patterns in flow persistence to within-watershed  
518 geological variability. The wettest locations are associated with portions of the stream network  
519 where past work has found significant exchange between limestone aquifers and the stream  
520 channel (Figure 6). In particular, we observed the highest flow persistence downstream of the  
521 Crouse Limestone, which has a high concentration of springs (Barry, 2018). Downstream of the  
522 Crouse limestone, flow persistence decreases are associated with the Morrill Limestone, which is  
523 a potential area of flow loss from the stream into the aquifer (Gambill et al., 2024). Past work,  
524 focused on tributary streamflow, has shown that the streamflow regime is primarily dominated  
525 by fill-and-spill dynamics, in which incoming precipitation largely contributes to increased  
526 subsurface storage until limestone aquifers are saturated and overflow to generate streamflow  
527 (Costigan et al., 2015). While flow at the watershed outlet tends to be dominated by groundwater  
528 (Hatley et al., 2023), there are relatively high fractions of young water (water that fell as  
529 precipitation within the past three months) throughout the stream network (Swenson et al., 2024).  
530 Therefore, our STIC data suggest an important role for fill-and-spill dynamics within specific  
531 limestone aquifers as key controls over flow persistence at fine spatial resolution within the  
532 stream network.  
533



534  
 535 **Figure 6. Spatial patterns of stream intermittency.** Map of the South Fork of Kings Creek watershed,  
 536 with each STIC location colored by the percentage of time it was classified as wet for the May 2021 to  
 537 May 2024 period of record. The white shaded bands show the estimated outcrop locations of the Crouse  
 538 (higher elevation) and Morrill (lower elevation) Limestone units based on elevation.

539  
 540 *3.5.2 Temporal intermittency dynamics*

541 The classified STIC data reveals a highly dynamic watershed that is rarely completely  
 542 wet and never completely dry (Figure 7a). Stream wetting tends to be flashy, with immediate  
 543 increases in the daily wet STIC proportion (defined as the proportion of total STIC readings that  
 544 are classified as wet on a given day) associated with precipitation events (Figure 7b), though  
 545 across our three-year study period the greatest wet STIC proportion tends to consistently occur in  
 546 the April-June timeframe. Following both seasonal and event-based peaks, the wet STIC  
 547 proportion gradually recedes back to a relatively consistent baseline of ~10-20% wet STICs,  
 548 which our spatial analysis shows are primarily concentrated in the middle portions of the  
 549 watershed (Figure 6).

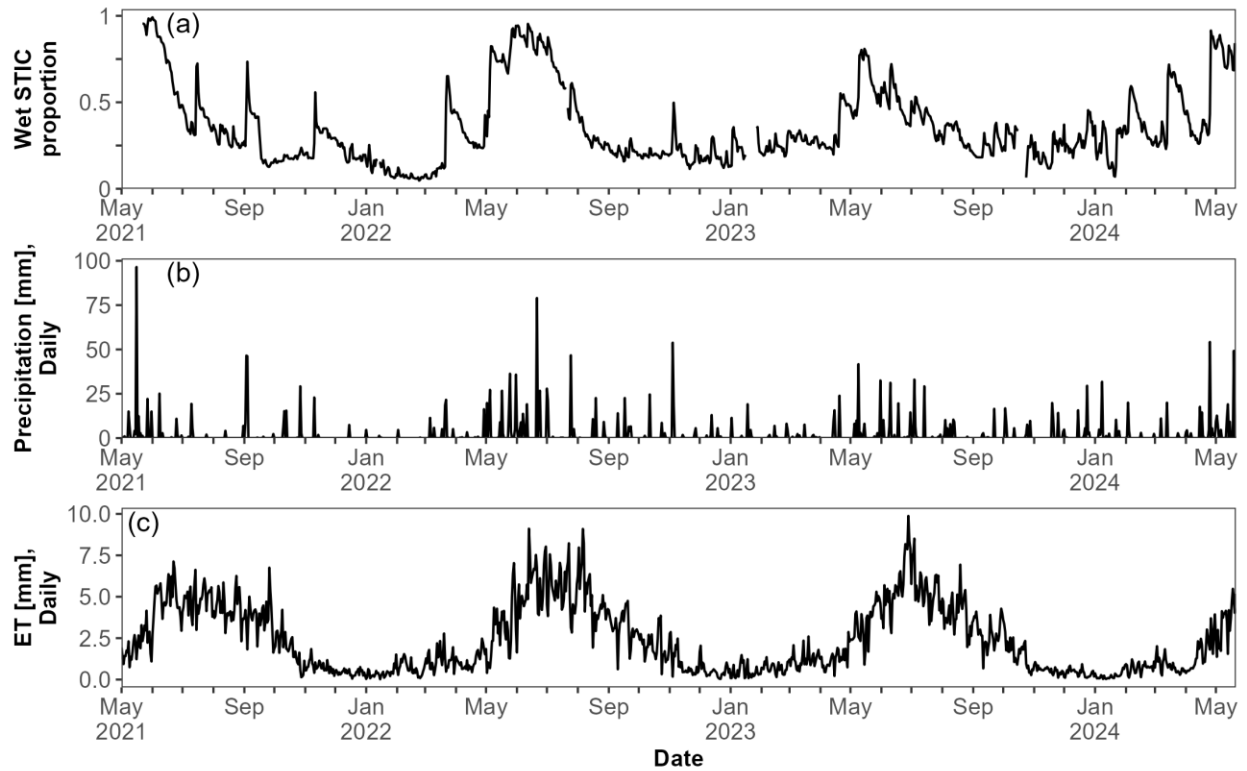
550 To investigate climatic drivers of intermittency, we obtained daily precipitation data from  
 551 the Konza Prairie LTER (Figure 7b; Nippert, 2024) and daily watershed-average  
 552 evapotranspiration (ET) data from OpenET (Figure 7c), which provides satellite-derived  
 553 estimates of daily ET for the western US (Melton et al., 2022; Volk et al., 2024). Precipitation  
 554 tends to be greatest during the March-July period, while ET is the greatest in the June-August  
 555 period (Figure 7b, Figure 7c). We tested the linear correlation between each of these climatic  
 556 drivers summed over time lags ranging from 1 to 365 days. The best predictive relationships for

557 wet STIC proportion occur when precipitation is summed over the prior 27 days ( $R^2 = 0.59$ ;  
558 Figure 8a, Figure 8d) and when ET is summed over the prior 290 days ( $R^2 = 0.57$ ; Figure 8b,  
559 Figure 8e). A simple multiple linear regression model (Eq. 1) using these two variables as  
560 predictors can explain 75% of the overall variability in wet STIC proportion (Figure 8c):  
561

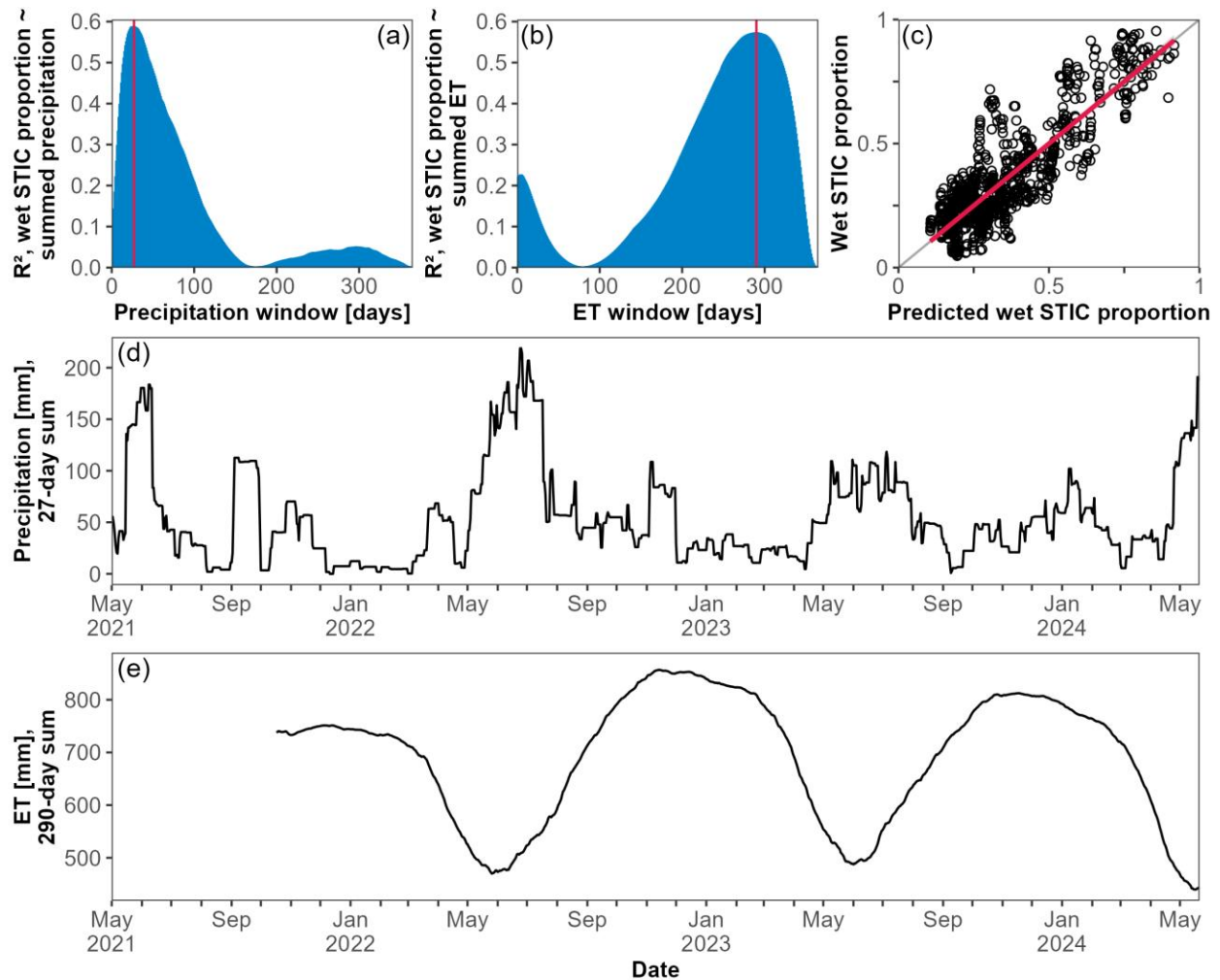
$$562 \quad WSP_D = 0.002574P_{27} - 0.000796ET_{290} + 0.757 \quad \{\text{Eq. 1}\}$$

563  
564 where  $WSP_D$  is the daily wet STIC proportion,  $P_{27}$  is the 27-day summed precipitation in mm,  
565 and  $ET_{290}$  is the 290-day summed ET in mm. Each of the predictors is statistically significant ( $p$   
566  $< 0.0001$ ).

567 These differing timescales for precipitation and ET correlations with wet STIC  
568 proportion reveal that temporal patterns of network-scale stream intermittency are strongly  
569 associated with the atmospheric water supply (precipitation) and losses (ET). Our results indicate  
570 that these two competing atmospheric and vegetative controls over water partitioning at the land  
571 surface are interacting over different timescales, with precipitation events leading to more rapid  
572 wetting throughout the watershed while the longer timescale for ET causes slower, gradual  
573 drying. While the ecoregion is native grassland, woody vegetation encroachment has expanded  
574 rapidly over the past several decades despite watershed burning and grazing, and has led to a  
575 decrease in annual streamflow and weakening relationship between precipitation and streamflow  
576 despite increasing precipitation (Keen et al., 2024; Sadayappan et al., 2023). Combined, this  
577 suggests that changes in the seasonality of precipitation or changes in growing season duration  
578 may lead to shifts in both hydrologic connectivity within the watershed and streamflow at the  
579 watershed outlet.  
580



581  
 582 **Figure 7. Temporal patterns of stream intermittency, precipitation, and ET.** (a) Daily wet STIC  
 583 precipitation proportion, (b) daily precipitation, and (c) daily ET for the May 2021 – May 2024 period (tick marks  
 584 show months).  
 585



586  
 587 **Figure 8. Evaluating timescales of links between driving variables and wet STIC proportion.**  $R^2$  of a  
 588 linear relationship between the proportion of wet STICs and (a) summed precipitation and (b) summer ET  
 589 for different windows. (c) Predicted wet STIC proportion from Eq. 1 based on precipitation over the  
 590 preceding 27-day window (best for from panel b;  $R^2 = 0.59$ ) and ET over the preceding 290-day window  
 591 (best for panel c;  $R^2 = 0.57$ ), with gray line showing 1:1 relationship and red line showing linear best fit  
 592 (overall  $R^2 = 0.75$ ). Daily time series of (d) summed 27-day precipitation and (e) summed 290-day ET.  
 593

## 594 4. Discussion

### 595 4.1 STICr functionality and future development needs

596 Although the package presented here represents an important step toward an open and  
597 reproducible framework for stream intermittency sensors, it is an ongoing package with several  
598 opportunities for improvement. First, while the *classify\_wetdry* function provides several  
599 different approaches to differentiate wet and dry sensor data, it does not currently take advantage  
600 of temperature data, which is an additional dataset recorded by STIC sensors that can be used for  
601 identifying dry and wet periods (Constantz et al., 2001). Second, STIC data can often have gaps  
602 due to sensor malfunction or loss, which can lead to difficulties in calculated derived metrics that  
603 depend on complete data such as communication distance (Aho, Kriloff et al., 2023),  
604 longitudinal connectivity (Zimmer and McGlynn, 2018), or active drainage density (Godsey and  
605 Kirchner, 2014). Work elsewhere has suggested that stream network length is often hierarchical,  
606 meaning that sites dry and rewet in a typical order (Botter et al., 2021; Botter and Durigetto,  
607 2020), and integrating this concept into STICr as a potential gap-filling approach (with  
608 appropriate flags in the QAQC column) would improve STICr's ability to develop spatially and  
609 temporally complete datasets of stream intermittency (Durigetto et al., 2023). Third, the  
610 package currently relies on manual reading and export of data from the proprietary HOBOWare  
611 format to a machine-readable CSV format. Development of a programming-based approach to  
612 read HOBOWare files directly would enhance reproducibility and efficiency. As an open-source  
613 package, we encourage STIC users to address these needs and/or make additional suggestions for  
614 improvements as issues on the package GitHub page ([https://github.com/HEAL-](https://github.com/HEAL-KGS/STICr/issues)  
615 [KGS/STICr/issues](https://github.com/HEAL-KGS/STICr/issues)) and contribute code they develop for their own analyses.

616

### 617 4.2 Integration into interdisciplinary research projects

618 Using STICr, we demonstrate how a workflow can be developed to create FAIR and  
619 standardized stream intermittency data for a project spanning multiple watersheds, institutions,  
620 and personnel (Figure 2). Since each watershed had different personnel, sensor deployment and  
621 maintenance timelines, and ability to access sites, the modular approach enabled by STICr  
622 allowed for the development of methodologically-consistent processing workflows with site-  
623 specific modifications where needed as the project evolved. Given the increasing  
624 interdisciplinary collaboration around non-perennial stream research, hydrological flow  
625 intermittence data is increasingly of interest to researchers in disciplines such as ecology (Allen  
626 et al., 2020; Datry et al., 2018; DelVecchia et al., 2022), and biogeochemistry (Price et al., 2024;  
627 Ward et al., 2019; Zimmer et al., 2022). Here, we demonstrate how STICr's functionality can be  
628 used to carry out sensitivity analyses and validations that quantify the impacts of different  
629 hydrologic data processing decisions on potential classification errors (Figure 4). These types of  
630 decisions are often hidden in derived data products, and STICr provides a quantitative  
631 framework that researchers can use to gather feedback and make collaborative decisions about  
632 data processing steps that meet the needs of eventual data users from other disciplines.  
633 Additionally, the standardized approach to QAQC flagging allows future users of the data,

634 whether within or beyond the project, to make important data filtering decisions and  
635 interpretations based on their research questions and data needs (Figure 5).

636

#### 637 *4.3 Evaluating spatial and temporal stream intermittency dynamics*

638 We also present a case study demonstrating how data processed using STICr can be used  
639 to assess spatial and temporal dynamics of stream intermittency in the South Fork Kings Creek  
640 watershed (Kansas, USA). We documented complex spatial patterns in watershed-scale stream  
641 intermittency (Figure 6), with the greatest wetness in the middle portion of the watershed and  
642 drier conditions upstream and downstream. We interpret these spatial patterns to be driven by  
643 localized stream-aquifer exchange that are ultimately controlled by the intersection of different  
644 limestone units with the stream channel (Gambill et al., 2024; Macpherson, 1996; Vero et al.,  
645 2018). This finding supports work done in sedimentary river systems documenting fine-scale  
646 variation in stream-aquifer exchange driven by streambed properties (Noorduijn et al., 2014;  
647 Shanafield et al., 2020b), and suggests that flow at the watershed outlet may not always be a  
648 direct indicator of hydrologic function, and associated water quality outcomes. As a result,  
649 network-scale stream connectivity indicators such as active channel length (Botter et al., 2021)  
650 and communication distance (Aho, Derryberry et al., 2023), informed by data from stream  
651 intermittency sensors like STICs, will likely play a critical role in determining the drivers of  
652 water quantity and quality impacts of non-perennial streams – a major open question in  
653 hydrologic research (Shanafield et al., 2020a; Zimmer et al., 2022).

654 Our investigation of temporal dynamics showed a time-varying meteorological response  
655 to controlling hydroclimatic variables, with a shorter (27-day) correlation with precipitation and  
656 a longer (290-day) correlation with ET in the watershed. These two timescales combined to  
657 produce rapid, precipitation event-driven wetting superimposed on a seasonal wetting and drying  
658 pattern created by the cumulative water use of vegetation throughout the summer and fall. This  
659 sheds light on climatic controlling the wetting and drying regime at this site, which have strong  
660 potential impacts on biogeochemical and ecological function (Price et al., 2024, 2021), and can  
661 vary at fine spatial scales (Sabathier et al., 2023). Both climate and land cover are changing in  
662 the region, with a long-term increasing precipitation trend counteracted by increased ET due to  
663 woody vegetation encroachment (Sadayappan et al., 2023). There is increasing evidence that  
664 non-perennial stream ecosystems can be characterized by alternative ecohydrological stable  
665 states (Ayers et al., 2024; Dodds et al., 2023; Heffernan, 2008; Popescu et al., 2022; Zipper et al.,  
666 2022) with nonlinear trajectories of change (Kar et al., 2024), suggesting that the interactions  
667 among concurrent changes in precipitation and ET could drive regime shifts to novel hydrologic  
668 regimes in the future.

669

## 670 **5. Conclusions**

671 We introduced STICr, an open-source R package for working with Stream Temperature,  
672 Intermittency, and Conductivity (STIC) data. STICr includes functions for tidying, calibrating,  
673 QAQCing, and validating STIC data to advance FAIR stream intermittency data. We then



674 provided a case study showing how STICr can be incorporated into a workflow for processing  
675 STIC data on a cross-regional interdisciplinary project, and how STICr capabilities related to  
676 validation and sensitivity analysis can be used to make data processing decisions that prioritize  
677 the needs to future data users. The stable version of STICr is currently available on the  
678 Comprehensive R Archive Network (CRAN; <https://cran.r-project.org/package=STICr>) and the  
679 development version is available on GitHub (<https://github.com/HEAL-KGS/STICr>) and we  
680 welcome contributions from the community.

681 For the South Fork Kings Creek watershed (Kansas, USA), we used the data produced by  
682 this workflow to show spatial and temporal dynamics of stream intermittency over a three-year  
683 study period. We found that the watershed stays wettest for the longest duration in the middle  
684 and western portions, which are areas where outcropping limestone aquifers intersect the aquifer.  
685 At the network-scale, we show that the proportion of the network that is wet at a daily timestep  
686 can be well-predicted by precipitation over an approximately monthly timescale (27 days) and  
687 ET over a longer period (290 days) that is associated with the cumulative water uptake by plants  
688 over the growing season. The contrast between shorter-term response to precipitation and longer-  
689 term response to ET leads to a hydrologic regime characterized by rapid increases in hydrologic  
690 connectivity in response to precipitation events and gradual recessions in response to seasonal  
691 network drying. The functions here, and associated shared workflows, provide a valuable basis  
692 for developing FAIR stream intermittency datasets and advancing links between non-perennial  
693 stream hydrology and other disciplines.

694

## 695 **Software and data availability**

- 696 • STICr:
  - 697 ○ Release version (v1.1): <https://cran.r-project.org/package=STICr>
  - 698 ○ Development version: <https://github.com/HEAL-KGS/STICr>
  - 699 ○ Archive version used in this manuscript:  
700 <https://hydroshare.org/resource/6044c6b7204e4013873f13b1a502e4a0/>
- 701 • AIMS STIC processing workflow:
  - 702 ○ Development version: [https://github.com/HEAL-KGS/AIMS\\_stic\\_pipeline](https://github.com/HEAL-KGS/AIMS_stic_pipeline)
  - 703 ○ Archive version used in this manuscript:  
704 <https://hydroshare.org/resource/6044c6b7204e4013873f13b1a502e4a0/>
- 705 • South Fork Kings Creek raw STIC data:  
706 <http://www.hydroshare.org/resource/77d68de62d6942ceab6859fc5541fd61> (Zipper et al.,  
707 2024)
- 708 • Code and data used to generate the figures in this manuscript:
  - 709 ○ Development version: [https://github.com/samzipper/AIMS\\_STIC\\_GP](https://github.com/samzipper/AIMS_STIC_GP)
  - 710 ○ Archive version used in this manuscript:  
711 <https://hydroshare.org/resource/6044c6b7204e4013873f13b1a502e4a0/>

712

713 **CRedit authorship contribution statement**

714 SZ: Conceptualization, Data curation, Formal analysis, Funding acquisition, Investigation,  
715 Methodology, Project administration, Resources, Software, Supervision, Validation,  
716 Visualization, Writing-Original Draft, Writing-Review & Editing

717  
718 CTW: Conceptualization, Data curation, Formal analysis, Investigation, Methodology, Software,  
719 Supervision, Validation, Visualization, Writing-Original Draft, Writing-Review & Editing

720  
721 DMP: Methodology, Software, Visualization, Writing-Review & Editing

722  
723 SCC: Data curation, Methodology, Software, Writing-Review & Editing

724  
725 SEG: Funding acquisition, Methodology, Supervision, Writing-Review & Editing

726  
727 KA: Funding acquisition, Methodology, Writing-Review & Editing

728

729 **Declaration of competing interest**

730 The authors declare no competing financial interests or personal relationships that could appear  
731 to influence the work reported in this paper.

732

733 **Acknowledgments**

734 This work was supported by National Science Foundation award OIA-2019603. We appreciate  
735 feedback on STICr code and use from Naomi Anderson, Anna Bergstrom, Connor Brown, Thane  
736 Kindred, Maggi Kraft, Alexi Sommerville, and the rest of the AIMS team. STICr and associated  
737 workflows make heavy use of the Tidyverse family of R packages (Wickham et al., 2019).

738

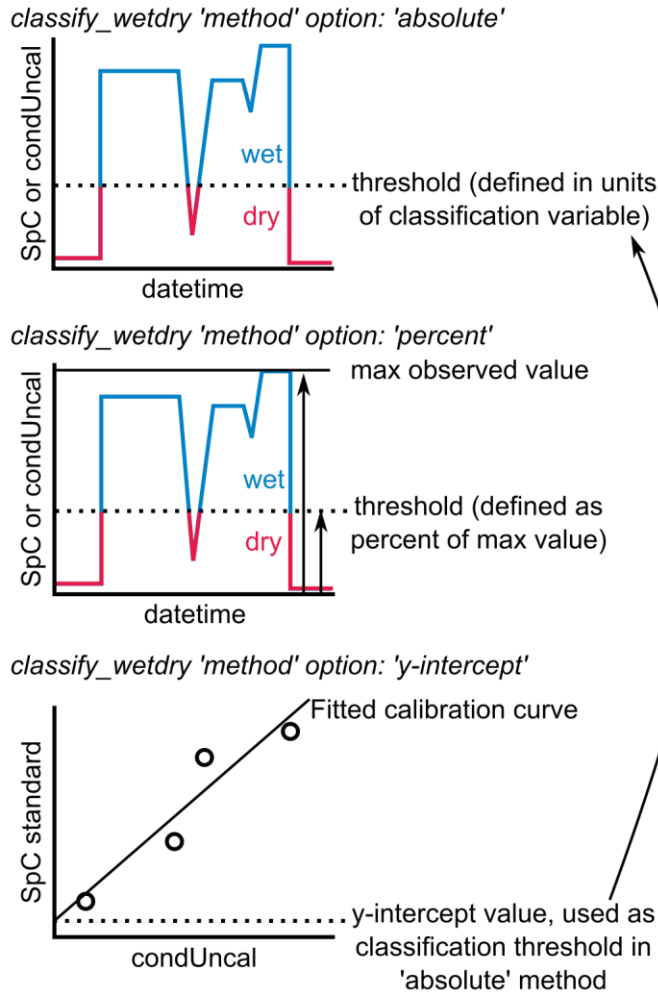
739 **Appendix 1: STIC qualitative rating criteria**

740 The following definitions were adopted by the AIMS project to rate the quality of STIC data for  
741 a given download period:

- 742
- 743 • **Excellent:** STIC was (1) calibrated prior to deployment, and (2) stayed operational  
744 throughout 95% of the download period, and (3) was not displaced from streambed (i.e.,  
745 the external electrodes were within 1 cm from stream bed at the time of download  
746 indicating minimal erosion/deposition), and (4) data from sensor roughly agree with field  
747 observations of wet/dry (i.e., >1000 Lux sensor reading on day of removal corresponds to  
748 field observations of water at STIC).
  - 749 • **Good:** (1) STIC stayed operational throughout the entire download period, and (2) the  
750 external electrodes were within 1 cm from stream bed at the time of download, and (3)  
751 data from sensor roughly agree with field observations of wet/dry, but (4) the STIC was  
not calibrated prior to deployment.

- 752 • **Fair:** (1) STIC stayed operational throughout 75% or more of the download period, and  
 753 (2) data roughly agree with field observations, and/or (3) the external electrodes were  
 754 between 1-3 cm from streambed at the time of download.
- 755 • **Poor:** (1) STIC stayed operational throughout less than 75% of the download period,  
 756 and/or (2) the external electrodes were >3 cm from streambed at the time of download,  
 757 and/or (3) data does NOT agree with field observations.

758 **Appendix 2: Visual representation of classify\_wetdry method options**



759 **Figure A1. Method options for STICr classify\_wetdry function.** The three current options for wetdry  
 760 classification are shown here. The option is selected by the user with the 'method' argument. For  
 761 'absolute' and 'percent' methods, an additional input for the 'threshold' is required. See Section 2.3 for  
 762 details.  
 763  
 764

765 **References**

- 766 Aho, K., Derryberry, D., Godsey, S.E., Ramos, R., Warix, S.R., Zipper, S., 2023.  
767 Communication Distance and Bayesian Inference in Non-Perennial Streams. *Water*  
768 *Resources Research* 59, e2023WR034513. <https://doi.org/10.1029/2023WR034513>
- 769 Aho, K., Kriloff, C., Godsey, S. E., Ramos, R., Wheeler, C., You, Y., et al. (2023). Non-  
770 perennial stream networks as directed acyclic graphs: The R-package streamDAG.  
771 *Environmental Modelling & Software*, 167, 105775.  
772 <https://doi.org/10.1016/j.envsoft.2023.105775>
- 773 Aho, K.S., Maavara, T., Cawley, K.M., Raymond, P.A., 2023. Inland Waters can Act as Nitrous  
774 Oxide Sinks: Observation and Modeling Reveal that Nitrous Oxide Undersaturation May  
775 Partially Offset Emissions. *Geophysical Research Letters* 50, e2023GL104987.  
776 <https://doi.org/10.1029/2023GL104987>
- 777 Allen, D.C., Datry, T., Boersma, K.S., Bogan, M.T., Boulton, A.J., Bruno, D., Busch, M.H.,  
778 Costigan, K.H., Dodds, W.K., Fritz, K.M., Godsey, S.E., Jones, J.B., Kaletova, T.,  
779 Kampf, S.K., Mims, M.C., Neeson, T.M., Olden, J.D., Pastor, A.V., Poff, N.L., Ruddell,  
780 B.L., Ruhi, A., Singer, G., Vezza, P., Ward, A.S., Zimmer, M., 2020. River ecosystem  
781 conceptual models and non-perennial rivers: A critical review. *WIREs Water* 7, e1473.  
782 <https://doi.org/10.1002/wat2.1473>
- 783 Ayers, J.R., Yarnell, S.M., Baruch, E., Lusardi, R.A., Grantham, T.E., 2024. Perennial and Non-  
784 Perennial Streamflow Regime Shifts Across California, USA. *Water Resources Research*  
785 60, e2023WR035768. <https://doi.org/10.1029/2023WR035768>
- 786 Barry, E. R. (2018). Characterizing Groundwater Flow through Merokarst, Northeast Kansas,  
787 USA (M.S. Thesis). University of Kansas, United States -- Kansas. Retrieved from  
788 [https://www.proquest.com/pqdtglobal/docview/2188065739/abstract/E714CD580E37463](https://www.proquest.com/pqdtglobal/docview/2188065739/abstract/E714CD580E374636PQ/1)  
789 6PQ/1
- 790 Beck, M.W., Schrandt, M.N., Wessel, M.R., Sherwood, E.T., Raulerson, G.E., Prasad, A.A.B.,  
791 Best, B.D., 2021. tbeptools: An R package for synthesizing estuarine data for  
792 environmental research. *Journal of Open Source Software* 6, 3485.  
793 <https://doi.org/10.21105/joss.03485>
- 794 Bilbrey, E.M., 2024. Quantifying Dissolved Organic Carbon Patterns and the Impact of Stream  
795 Network Connectivity on Export From Semi-Arid Intermittent Watersheds (M.S.). Idaho  
796 State University, United States -- Idaho.
- 797 Boersch-Supan, P., Petry, W., 2018. microclimloggers.
- 798 Bolotin, L.A., Summers, B.M., Savoy, P., Blaszczyk, J.R., 2023. Classifying freshwater salinity  
799 regimes in central and western U.S. streams and rivers. *Limnology and Oceanography*  
800 *Letters* 8, 103–111. <https://doi.org/10.1002/lol2.10251>
- 801 Botter, G., Durighetto, N., 2020. The Stream Length Duration Curve: A Tool for Characterizing  
802 the Time Variability of the Flowing Stream Length. *Water Resources Research* 56,  
803 e2020WR027282. <https://doi.org/10.1029/2020WR027282>
- 804 Botter, G., Vingiani, F., Senatore, A., Jensen, C., Weiler, M., McGuire, K., Mendicino, G.,  
805 Durighetto, N., 2021. Hierarchical climate-driven dynamics of the active channel length  
806 in temporary streams. *Sci Rep* 11, 21503. <https://doi.org/10.1038/s41598-021-00922-2>
- 807 Brinkerhoff, C.B., Gleason, C.J., Kotchen, M.J., Kysar, D.A., Raymond, P.A., 2024. Ephemeral  
808 stream water contributions to United States drainage networks. *Science* 384, 1476–1482.  
809 <https://doi.org/10.1126/science.adg9430>
- 810 Burke, E., Wilhelm, J., Zipper, S., Brown, C., 2024. AIMS SOP STIC Calibration.

811 Busch, M.H., Boersma, K.S., Cook, S.C., Jones, C.N., Loflen, C., Mazor, R.D., Stancheva, R.,  
812 Price, A.N., Stubbington, R., Zimmer, M.A., Allen, D.C., 2024. Macroinvertebrate, algal  
813 and diatom assemblages respond differently to both drying and wetting transitions in non-  
814 perennial streams. *Freshwater Biology* 69, 1568–1582. <https://doi.org/10.1111/fwb.14327>

815 Chapin, T.P., Todd, A.S., Zeigler, M.P., 2014. Robust, low-cost data loggers for stream  
816 temperature, flow intermittency, and relative conductivity monitoring. *Water Resour.*  
817 *Res.* n/a-n/a. <https://doi.org/10.1002/2013WR015158>

818 Constantz, J., Stonestorm, D., Stewart, A.E., Niswonger, R., Smith, T.R., 2001. Analysis of  
819 streambed temperatures in ephemeral channels to determine streamflow frequency and  
820 duration. *Water Resources Research* 37, 317–328.  
821 <https://doi.org/10.1029/2000WR900271>

822 Costigan, K.H., Daniels, M.D., Dodds, W.K., 2015. Fundamental spatial and temporal  
823 disconnections in the hydrology of an intermittent prairie headwater network. *Journal of*  
824 *Hydrology* 522, 305–316. <https://doi.org/10.1016/j.jhydrol.2014.12.031>

825 Datry, T., Foulquier, A., Corti, R., von Schiller, D., Tockner, K., Mendoza-Lera, C., Clément,  
826 J.C., Gessner, M.O., Moleón, M., Stubbington, R., Gücker, B., Albariño, R., Allen, D.C.,  
827 Altermatt, F., Arce, M.I., Arnon, S., Banas, D., Banegas-Medina, A., Beller, E.,  
828 Blanchette, M.L., Blanco-Libreros, J.F., Blessing, J.J., Boëchat, I.G., Boersma, K.S.,  
829 Bogan, M.T., Bonada, N., Bond, N.R., Brintrup Barría, K.C., Bruder, A., Burrows, R.M.,  
830 Cancellario, T., Canhoto, C., Carlson, S.M., Cauvy-Fraunié, S., Cid, N., Danger, M., de  
831 Freitas Terra, B., De Girolamo, A.M., de La Barra, E., del Campo, R., Diaz-Villanueva,  
832 V.D., Dyer, F., Elosegí, A., Faye, E., Febria, C., Four, B., Gafny, S., Ghate, S.D., Gómez,  
833 R., Gómez-Gener, L., Graça, M.A.S., Guareschi, S., Hoppeler, F., Hwan, J.L., Jones, J.I.,  
834 Kubheka, S., Laini, A., Langhans, S.D., Leigh, C., Little, C.J., Lorenz, S., Marshall, J.C.,  
835 Martín, E., McIntosh, A.R., Meyer, E.I., Miliša, M., Mlambo, M.C., Morais, M., Moya,  
836 N., Negus, P.M., Niyogi, D.K., Papatheodoulou, A., Pardo, I., Pařil, P., Pauls, S.U.,  
837 Pešić, V., Poláček, M., Robinson, C.T., Rodríguez-Lozano, P., Rolls, R.J., Sánchez-  
838 Montoya, M.M., Savić, A., Shumilova, O., Sridhar, K.R., Steward, A.L., Storey, R.,  
839 Taleb, A., Uzan, A., Vander Vorste, R., Waltham, N.J., Woelfle-Erskine, C., Zak, D.,  
840 Zarfl, C., Zoppini, A., 2018. A global analysis of terrestrial plant litter dynamics in non-  
841 perennial waterways. *Nature Geosci* 11, 497–503. [https://doi.org/10.1038/s41561-018-](https://doi.org/10.1038/s41561-018-0134-4)  
842 [0134-4](https://doi.org/10.1038/s41561-018-0134-4)

843 DeCicco, L., Hirsch, R., Lorenz, D., Read, J., Walker, J., Platt, L., Watkins, D., Blodgett, D.,  
844 Johnson, M., Krall, A., Stanish, L., 2024. dataRetrieval: R packages for discovering and  
845 retrieving water data available from U.S. federal hydrologic web services.  
846 <https://doi.org/10.5066/P9X4L3GE>

847 DelVecchia, A.G., Shanafield, M., Zimmer, M.A., Busch, M.H., Krabbenhoft, C.A.,  
848 Stubbington, R., Kaiser, K.E., Burrows, R.M., Hosen, J., Datry, T., Kampf, S.K., Zipper,  
849 S.C., Fritz, K., Costigan, K., Allen, D.C., 2022. Reconceptualizing the hyporheic zone for  
850 nonperennial rivers and streams. *Freshwater Science* 000–000.  
851 <https://doi.org/10.1086/720071>

852 Dempsey, D., 2024. sensorstrings.

853 Dodds, W.K., Ratajczak, Z., Keen, R.M., Nippert, J.B., Grudzinski, B., Veach, A., Taylor, J.H.,  
854 Kuhl, A., 2023. Trajectories and state changes of a grassland stream and riparian zone  
855 after a decade of woody vegetation removal. *Ecological Applications* 33, e2830.  
856 <https://doi.org/10.1002/eap.2830>

857 Durand, M., 2020. TDPanalysis: Granier's Sap Flow Sensors (TDP) Analysis.

858 Durighetto, N., Noto, S., Tauro, F., Grimaldi, S., Botter, G., 2023. Integrating spatially-and  
859 temporally-heterogeneous data on river network dynamics using graph theory. *iScience*  
860 26. <https://doi.org/10.1016/j.isci.2023.107417>

861 Gama, J., 2015. thermocouple: Temperature Measurement with Thermocouples, RTD and IC  
862 Sensors.

863 Gambill, I., Zipper, S., Kirk, M.F., Seybold, E.C., 2024. Exploring drivers of groundwater  
864 recharge at Konza Prairie (Flint Hills region, Kansas, USA) using transfer function noise  
865 models (KGS Open-File Report 2024-6 No. 2024-6). Kansas Geological Survey,  
866 Lawrence KS.

867 Godsey, S., Wheeler, C., Zipper, S., 2024. AIMS SOP STIC Deployment and Maintenance.

868 Godsey, S.E., Kirchner, J.W., 2014. Dynamic, discontinuous stream networks: hydrologically  
869 driven variations in active drainage density, flowing channels and stream order.  
870 *Hydrological Processes* 28, 5791–5803. <https://doi.org/10.1002/hyp.10310>

871 Golden, H. E., Christensen, J. R., McMillan, H. K., Kelleher, C. A., Lane, C. R., Husic, A., et al.  
872 (2025). Advancing the science of headwater streamflow for global water protection.  
873 *Nature Water*, 1–11. <https://doi.org/10.1038/s44221-024-00351-1>

874 Hale, R.L., Godsey, S.E., 2019. Dynamic stream network intermittence explains emergent  
875 dissolved organic carbon chemostasis in headwaters. *Hydrological Processes* 33, 1926–  
876 1936. <https://doi.org/10.1002/hyp.13455>

877 Hale, R.L., Godsey, S.E., Dohman, J.M., Warix, S.R., 2024. Diel dissolved organic matter  
878 patterns reflect spatiotemporally varying sources and transformations along an  
879 intermittent stream. *Limnology and Oceanography*. <https://doi.org/10.1002/lno.12695>

880 Hall, C.A., Saia, S.M., Popp, A.L., Dogulu, N., Schymanski, S.J., Drost, N., van Emmerik, T.,  
881 Hut, R., 2022. A hydrologist's guide to open science. *Hydrology and Earth System*  
882 *Sciences* 26, 647–664. <https://doi.org/10.5194/hess-26-647-2022>

883 Hatley, C.M., Armijo, B., Andrews, K., Anhold, C., Nippert, J.B., Kirk, M.F., 2023. Intermittent  
884 streamflow generation in a merokarst headwater catchment. *Environmental Science:*  
885 *Advances* 2, 115–131. <https://doi.org/10.1039/D2VA00191H>

886 Heffernan, J.B., 2008. Wetlands as an Alternative Stable State in Desert Streams. *Ecology* 89,  
887 1261–1271. <https://doi.org/10.1890/07-0915.1>

888 Jensen, C.K., McGuire, K.J., McLaughlin, D.L., Scott, D.T., 2019. Quantifying spatiotemporal  
889 variation in headwater stream length using flow intermittency sensors. *Environ Monit*  
890 *Assess* 191, 226. <https://doi.org/10.1007/s10661-019-7373-8>

891 Kaletová, T., Loures, L., Castanho, R.A., Aydin, E., Gama, J.T. da, Loures, A., Truchy, A.,  
892 2019. Relevance of Intermittent Rivers and Streams in Agricultural Landscape and Their  
893 Impact on Provided Ecosystem Services—A Mediterranean Case Study. *International*  
894 *Journal of Environmental Research and Public Health* 16, 2693.  
895 <https://doi.org/10.3390/ijerph16152693>

896 Kar, K.K., Roy, T., Zipper, S., Godsey, S.E., 2024. Nonlinear trends in signatures characterizing  
897 non-perennial US streams. *Journal of Hydrology* 635, 131131.  
898 <https://doi.org/10.1016/j.jhydrol.2024.131131>

899 Keen, R.M., Sadayappan, K., Jarecke, K.M., Li, L., Kirk, M.F., Sullivan, P.L., Nippert, J.B.,  
900 2024. Unexpected hydrologic response to ecosystem state change in tallgrass prairie.  
901 *Journal of Hydrology* 643, 131937. <https://doi.org/10.1016/j.jhydrol.2024.131937>

902 Kindred, T., 2022. Spatial Structure, Temporal Patterns, and Drivers of Stream Drying in the  
903 Gibson Jack Watershed, Bannock County, Idaho (M.S.). Idaho State University, United  
904 States -- Idaho.

905 Krabbenhoft, C.A., Allen, G.H., Lin, P., Godsey, S.E., Allen, D.C., Burrows, R.M., DelVecchia,  
906 A.G., Fritz, K.M., Shanafield, M., Burgin, A.J., Zimmer, M.A., Datry, T., Dodds, W.K.,  
907 Jones, C.N., Mims, M.C., Franklin, C., Hammond, J.C., Zipper, S., Ward, A.S., Costigan,  
908 K.H., Beck, H.E., Olden, J.D., 2022. Assessing placement bias of the global river gauge  
909 network. *Nat Sustain* 1–7. <https://doi.org/10.1038/s41893-022-00873-0>

910 Macpherson, G.L., 1996. Hydrogeology of thin limestones: the Konza Prairie Long-Term  
911 Ecological Research Site, Northeastern Kansas. *Journal of Hydrology* 186, 191–228.  
912 [https://doi.org/10.1016/S0022-1694\(96\)03029-6](https://doi.org/10.1016/S0022-1694(96)03029-6)

913 Malish, M.C., Gao, S., Allen, D.C., Neeson, T.M., 2024. Impacts of stream drying depend on  
914 stream network size and location of drying. *Ecological Applications* 34, e3015.  
915 <https://doi.org/10.1002/eap.3015>

916 Melton, F.S., Huntington, J., Grimm, R., Herring, J., Hall, M., Rollison, D., Erickson, T., Allen,  
917 R., Anderson, M., Fisher, J.B., Kilic, A., Senay, G.B., Volk, J., Hain, C., Johnson, L.,  
918 Ruhoff, A., Blankenau, P., Bromley, M., Carrara, W., Daudert, B., Doherty, C.,  
919 Dunkerly, C., Friedrichs, M., Guzman, A., Halverson, G., Hansen, J., Harding, J., Kang,  
920 Y., Ketchum, D., Minor, B., Morton, C., Ortega-Salazar, S., Ott, T., Ozdogan, M.,  
921 ReVelle, P.M., Schull, M., Wang, C., Yang, Y., Anderson, R.G., 2022. OpenET: Filling a  
922 Critical Data Gap in Water Management for the Western United States. *JAWRA Journal*  
923 *of the American Water Resources Association* 58, 971–994.  
924 <https://doi.org/10.1111/1752-1688.12956>

925 Messenger, M.L., Lehner, B., Cockburn, C., Lamouroux, N., Pella, H., Snelder, T., Tockner, K.,  
926 Trautmann, T., Watt, C., Datry, T., 2021. Global prevalence of non-perennial rivers and  
927 streams. *Nature* 594, 391–397. <https://doi.org/10.1038/s41586-021-03565-5>

928 Milford, C., Truong, B., 2024. Smart Rock [WWW Document]. URL  
929 <https://github.com/OPENSLab-OSU/SmartRock?tab=readme-ov-file>

930 Newcomb, S.K., Godsey, S.E., 2023. Nonlinear Riparian Interactions Drive Changes in  
931 Headwater Streamflow. *Water Resources Research* 59, e2023WR034870.  
932 <https://doi.org/10.1029/2023WR034870>

933 Nippert, J.B., 2024. AWE01 Meteorological data from the konza prairie headquarters weather  
934 station. <https://doi.org/10.6073/pasta/910469efbf1f7e8d54c2b1ca864edec9>

935 Noorduijn, S.L., Shanafield, M., Trigg, M.A., Harrington, G.A., Cook, P.G., Peeters, L., 2014.  
936 Estimating seepage flux from ephemeral stream channels using surface water and  
937 groundwater level data. *Water Resources Research* 50, 1474–1489.  
938 <https://doi.org/10.1002/2012WR013424>

939 Paillex, A., Siebers, A.R., Ebi, C., Mesman, J., Robinson, C.T., 2020. High stream intermittency  
940 in an alpine fluvial network: Val Roseg, Switzerland. *Limnology and Oceanography* 65,  
941 557–568. <https://doi.org/10.1002/lno.11324>

942 Peterson, D.M., Flynn, S.M., Lanfear, R.S., Smith, C., Swenson, L.J., Belskis, A.M., Cook, S.C.,  
943 Wheeler, C.T., Wilhelm, J.F., Burgin, A.J., 2023. Team science: A syllabus for success  
944 on big projects. *Ecology and Evolution* 13, e10343. <https://doi.org/10.1002/ece3.10343>

945 Popescu, I., Zipper, S., & Seybold, E. (2022). Identifying Regime Shifts in the Arkansas River  
946 Near Larned, Kansas (KGS Open-File Report No. 2022–4) (p. 27). Lawrence KS: Kansas

947 Geological Survey. Retrieved from  
 948 <https://www.kgs.ku.edu/Publications/OFR/2022/OFR2022-4/index.html>

949 Price, A.N., Jones, C.N., Hammond, J.C., Zimmer, M.A., Zipper, S.C., 2021. The Drying  
 950 Regimes of Non-Perennial Rivers and Streams. *Geophysical Research Letters* 48,  
 951 e2021GL093298. <https://doi.org/10.1029/2021GL093298>

952 Price, A.N., Zimmer, M.A., Bergstrom, A., Burgin, A.J., Seybold, E.C., Krabbenhoft, C.A.,  
 953 Zipper, S., Busch, M.H., Dodds, W.K., Walters, A., Rogosch, J.S., Stubbington, R.,  
 954 Walker, R.H., Stegen, J.C., Datry, T., Messenger, M., Olden, J., Godsey, S.E., Shanafield,  
 955 M., Lytle, D., Burrows, R., Kaiser, K.E., Allen, G.H., Mims, M.C., Tonkin, J.D., Bogan,  
 956 M., Hammond, J.C., Boersma, K., Myers-Pigg, A.N., DelVecchia, A., Allen, D., Yu, S.,  
 957 Ward, A., 2024. Biogeochemical and community ecology responses to the wetting of  
 958 non-perennial streams. *Nat Water* 2, 815–826. [https://doi.org/10.1038/s44221-024-](https://doi.org/10.1038/s44221-024-00298-3)  
 959 00298-3

960 Read, J.S., Garner, B., Pellerin, B., Loken, L., 2015. sensorQC.

961 Reinecke, R., Trautmann, T., Wagener, T., Schüler, K., 2022. The critical need to foster  
 962 computational reproducibility. *Environ. Res. Lett.* 17, 041005.  
 963 <https://doi.org/10.1088/1748-9326/ac5cf8>

964 Sabathier, R., Singer, M.B., Stella, J.C., Roberts, D.A., Caylor, K.K., Jaeger, K.L., Olden, J.D.,  
 965 2023. High resolution spatiotemporal patterns of flow at the landscape scale in montane  
 966 non-perennial streams. *River Research and Applications* 39, 225–240.  
 967 <https://doi.org/10.1002/rra.4076>

968 Sadayappan, K., Keen, R., Jarecke, K.M., Moreno, V., Nippert, J.B., Kirk, M.F., Sullivan, P.L.,  
 969 Li, L., 2023. Drier streams despite a wetter climate in woody-encroached grasslands.  
 970 *Journal of Hydrology* 130388. <https://doi.org/10.1016/j.jhydrol.2023.130388>

971 Sauquet, E., Shanafield, M., Hammond, J., Sefton, C., Leigh, C., Datry, T., 2021. Classification  
 972 and trends in intermittent river flow regimes in Australia, northwestern Europe and USA:  
 973 a global perspective. *Journal of Hydrology* 126170.  
 974 <https://doi.org/10.1016/j.jhydrol.2021.126170>

975 Seybold, E.C., Bergstrom, A., Jones, C.N., Burgin, A.J., Zipper, S., Godsey, S.E., Dodds, W.K.,  
 976 Zimmer, M.A., Shanafield, M., Datry, T., Mazor, R.D., Messenger, M.L., Olden, J.D.,  
 977 Ward, A., Yu, S., Kaiser, K.E., Shogren, A., Walker, R.H., 2023. How low can you go?  
 978 Widespread challenges in measuring low stream discharge and a path forward.  
 979 *Limnology and Oceanography Letters* 8, 804–811. <https://doi.org/10.1002/lol2.10356>

980 Shanafield, M., Bourke, S.A., Zimmer, M.A., Costigan, K.H., 2020a. An overview of the  
 981 hydrology of non-perennial rivers and streams. *WIREs Water* 8, e1504.  
 982 <https://doi.org/10.1002/wat2.1504>

983 Shanafield, M., Cook, P.G., 2014. Transmission losses, infiltration and groundwater recharge  
 984 through ephemeral and intermittent streambeds: A review of applied methods. *Journal of*  
 985 *Hydrology* 511, 518–529. <https://doi.org/10.1016/j.jhydrol.2014.01.068>

986 Shanafield, M., Gutiérrez-Jurado, K., White, N., Hatch, M., Keane, R., 2020b. Catchment-Scale  
 987 Characterization of Intermittent Stream Infiltration; a Geophysics Approach. *Journal of*  
 988 *Geophysical Research: Earth Surface* 125, e2019JF005330.  
 989 <https://doi.org/10.1029/2019JF005330>

990 Shaughnessy, A., Prener, C., Hasenmueller, E., 2018. driftR.  
 991 <https://doi.org/10.5281/zenodo.1288819>



992 Stagge, J.H., Rosenberg, D.E., Abdallah, A.M., Akbar, H., Attallah, N.A., James, R., 2019.  
 993 Assessing data availability and research reproducibility in hydrology and water resources.  
 994 Scientific Data 6, 190030. <https://doi.org/10.1038/sdata.2019.30>

995 Stubbington, R., Acreman, M., Acuña, V., Boon, P.J., Boulton, A.J., England, J., Gilvear, D.,  
 996 Sykes, T., Wood, P.J., 2020. Ecosystem services of temporary streams differ between wet  
 997 and dry phases in regions with contrasting climates and economies. *People and Nature* 2,  
 998 660–677. <https://doi.org/10.1002/pan3.10113>

999 Sullivan, P.L., Zhang, C., Behm, M., Zhang, F., Macpherson, G.L., 2020. Toward a new  
 1000 conceptual model for groundwater flow in merokarst systems: Insights from multiple  
 1001 geophysical approaches. *Hydrological Processes* 34, 4697–4711.  
 1002 <https://doi.org/10.1002/hyp.13898>

1003 Swenson, L.J., Zipper, S., Peterson, D.M., Jones, C.N., Burgin, A.J., Seybold, E., Kirk, M.F.,  
 1004 Hatley, C., 2024. Changes in Water Age During Dry-Down of a Non-Perennial Stream.  
 1005 *Water Resources Research* 60, e2023WR034623.  
 1006 <https://doi.org/10.1029/2023WR034623>

1007 Trambly, Y., Rutkowska, A., Sauquet, E., Sefton, C., Laaha, G., Osuch, M., Albuquerque, T.,  
 1008 Alves, M.H., Banasik, K., Beaufort, A., Brocca, L., Camici, S., Csabai, Z., Dakhlaoui, H.,  
 1009 DeGirolamo, A.M., Dörflinger, G., Gallart, F., Gauster, T., Hanich, L., Kohnová, S.,  
 1010 Mediero, L., Plamen, N., Parry, S., Quintana-Seguí, P., Tzoraki, O., Datry, T., 2021.  
 1011 Trends in flow intermittence for European rivers. *Hydrological Sciences Journal* 66, 37–  
 1012 49. <https://doi.org/10.1080/02626667.2020.1849708>

1013 Vero, S.E., Macpherson, G.L., Sullivan, P.L., Brookfield, A.E., Nippert, J.B., Kirk, M.F., Datta,  
 1014 S., Kempton, P., 2018. Developing a Conceptual Framework of Landscape and  
 1015 Hydrology on Tallgrass Prairie: A Critical Zone Approach. *Vadose Zone Journal* 17, 0.  
 1016 <https://doi.org/10.2136/vzj2017.03.0069>

1017 Volk, J.M., Huntington, J.L., Melton, F.S., Allen, R., Anderson, M., Fisher, J.B., Kilic, A.,  
 1018 Ruhoff, A., Senay, G.B., Minor, B., Morton, C., Ott, T., Johnson, L., Comini de Andrade,  
 1019 B., Carrara, W., Doherty, C.T., Dunkerly, C., Friedrichs, M., Guzman, A., Hain, C.,  
 1020 Halverson, G., Kang, Y., Knipper, K., Laipelt, L., Ortega-Salazar, S., Pearson, C.,  
 1021 Parrish, G.E.L., Purdy, A., ReVelle, P., Wang, T., Yang, Y., 2024. Assessing the  
 1022 accuracy of OpenET satellite-based evapotranspiration data to support water resource and  
 1023 land management applications. *Nat Water* 1–13. <https://doi.org/10.1038/s44221-023-00181-7>

1024

1025 Ward, A.S., Zarnetske, J.P., Baranov, V., Blaen, P.J., Brekenfeld, N., Chu, R., Derelle, R.,  
 1026 Drummond, J., Fleckenstein, J.H., Garayburu-Caruso, V., Graham, E., Hannah, D.,  
 1027 Harman, C.J., Herzog, S., Hixson, J., Knapp, J.L.A., Krause, S., Kurz, M.J.,  
 1028 Lewandowski, J., Li, A., Martí, E., Miller, M., Milner, A.M., Neil, K., Orsini, L.,  
 1029 Packman, A.I., Plont, S., Renteria, L., Roche, K., Royer, T., Schmadel, N.M., Segura, C.,  
 1030 Stegen, J., Toyoda, J., Wells, J., Wisnoski, N.I., Wondzell, S.M., 2019. Co-located  
 1031 contemporaneous mapping of morphological, hydrological, chemical, and biological  
 1032 conditions in a 5th-order mountain stream network, Oregon, USA. *Earth System Science*  
 1033 *Data* 11, 1567–1581. <https://doi.org/10.5194/essd-11-1567-2019>

1034 Warix, S.R., Godsey, S.E., Flerchinger, G., Havens, S., Lohse, K.A., Bottenberg, H.C., Chu, X.,  
 1035 Hale, R.L., Seyfried, M., 2023. Evapotranspiration and groundwater inputs control the  
 1036 timing of diel cycling of stream drying during low-flow periods. *Front. Water* 5.  
 1037 <https://doi.org/10.3389/frwa.2023.1279838>

1038 Warix, S.R., Godsey, S.E., Lohse, K.A., Hale, R.L., 2021. Influence of groundwater and  
1039 topography on stream drying in semi-arid headwater streams. *Hydrological Processes* 35,  
1040 e14185. <https://doi.org/10.1002/hyp.14185>

1041 Wickham, H., Averick, M., Bryan, J., Chang, W., McGowan, L.D., François, R., Grolemund, G.,  
1042 Hayes, A., Henry, L., Hester, J., Kuhn, M., Pedersen, T.L., Miller, E., Bache, S.M.,  
1043 Müller, K., Ooms, J., Robinson, D., Seidel, D.P., Spinu, V., Takahashi, K., Vaughan, D.,  
1044 Wilke, C., Woo, K., Yutani, H., 2019. Welcome to the Tidyverse. *Journal of Open*  
1045 *Source Software* 4, 1686. <https://doi.org/10.21105/joss.01686>

1046 Wilkinson, M.D., Dumontier, M., Aalbersberg, I.J., Appleton, G., Axton, M., Baak, A.,  
1047 Blomberg, N., Boiten, J.-W., Santos, L.B. da S., Bourne, P.E., Bouwman, J., Brookes,  
1048 A.J., Clark, T., Crosas, M., Dillo, I., Dumon, O., Edmunds, S., Evelo, C.T., Finkers, R.,  
1049 Gonzalez-Beltran, A., Gray, A.J.G., Groth, P., Goble, C., Grethe, J.S., Heringa, J., Hoen,  
1050 P.A.C. 't, Hooft, R., Kuhn, T., Kok, R., Kok, J., Lusher, S.J., Martone, M.E., Mons, A.,  
1051 Packer, A.L., Persson, B., Rocca-Serra, P., Roos, M., Schaik, R. van, Sansone, S.-A.,  
1052 Schultes, E., Sengstag, T., Slater, T., Strawn, G., Swertz, M.A., Thompson, M., Lei, J.  
1053 van der, Mulligen, E. van, Velterop, J., Waagmeester, A., Wittenburg, P., Wolstencroft,  
1054 K., Zhao, J., Mons, B., 2016. The FAIR Guiding Principles for scientific data  
1055 management and stewardship. *Scientific Data* 3, 160018.  
1056 <https://doi.org/10.1038/sdata.2016.18>

1057 Zimmer, M.A., Burgin, A.J., Kaiser, K., Hosen, J., 2022. The unknown biogeochemical impacts  
1058 of drying rivers and streams. *Nat Commun* 13, 7213. [https://doi.org/10.1038/s41467-022-](https://doi.org/10.1038/s41467-022-34903-4)  
1059 [34903-4](https://doi.org/10.1038/s41467-022-34903-4)

1060 Zimmer, M.A., McGlynn, B.L., 2018. Lateral, Vertical, and Longitudinal Source Area  
1061 Connectivity Drive Runoff and Carbon Export Across Watershed Scales. *Water*  
1062 *Resources Research* 54, 1576–1598. <https://doi.org/10.1002/2017WR021718>

1063 Zipper, S., Popescu, I., Compare, K., Zhang, C., Seybold, E.C., 2022. Alternative stable states  
1064 and hydrological regime shifts in a large intermittent river. *Environ. Res. Lett.* 17,  
1065 074005. <https://doi.org/10.1088/1748-9326/ac7539>

1066 Zipper, S., Wheeler, C., Somerville, A., 2024. Kings Creek (Konza Prairie) Stream Temperature,  
1067 Intermittency, and Conductivity Data (AIMS\_GP\_KNZ\_approach1\_STIC).

1068 Zipper, S.C., Hammond, J.C., Shanafield, M., Zimmer, M., Datry, T., Jones, C.N., Kaiser, K.E.,  
1069 Godsey, S.E., Burrows, R.M., Blaszcak, J.R., Busch, M.H., Price, A.N., Boersma, K.S.,  
1070 Ward, A.S., Costigan, K., Allen, G.H., Krabbenhoft, C.A., Dodds, W.K., Mims, M.C.,  
1071 Olden, J.D., Kampf, S.K., Burgin, A.J., Allen, D.C., 2021. Pervasive changes in stream  
1072 intermittency across the United States. *Environ. Res. Lett.* 16, 084033.  
1073 <https://doi.org/10.1088/1748-9326/ac14ec>

1074 Zipper, S.C., Stack Whitney, K., Deines, J.M., Befus, K.M., Bhatia, U., Albers, S.J., Beecher, J.,  
1075 Brelsford, C., Garcia, M., Gleeson, T., O'Donnell, F., Resnik, D., Schlager, E., 2019.  
1076 Balancing Open Science and Data Privacy in the Water Sciences. *Water Resources*  
1077 *Research* 55, 5202–5211. <https://doi.org/10.1029/2019WR025080>

1078  
1079